

Synthetic Augmentation in Imbalanced Learning: When It Helps, When It Hurts, and How Much to Add

Zhengchi Ma* and Anru R. Zhang†

Abstract

Imbalanced classification, where one class is observed far less frequently than the other, often causes standard training procedures to prioritize the majority class and perform poorly on rare but important cases. A classic and widely used remedy is to augment the minority class with synthetic examples, but two basic questions remain under-resolved: when does synthetic augmentation actually help, and how many synthetic samples should be generated?

We develop a unified statistical framework for synthetic augmentation in imbalanced learning, studying models trained on imbalanced data augmented with synthetic minority samples and evaluated under the balanced population risk. Our theory shows that synthetic data is not always beneficial. In a “local symmetry” regime, imbalance is not the dominant source of error near the balanced optimum, so adding synthetic samples cannot improve learning rates and can even degrade performance by amplifying generator mismatch. When augmentation can help (a “local asymmetry” regime), the optimal synthetic size depends on generator accuracy and on whether the generator’s residual mismatch is directionally aligned with the intrinsic majority–minority shift. This structure can make the best synthetic size deviate from naive full balancing, sometimes by a small refinement and sometimes substantially when generator bias is systematic. Practically, we recommend Validation-Tuned Synthetic Size (VTSS): select the synthetic size by minimizing balanced validation loss over a range centered near the fully balanced baseline, while allowing meaningful departures when the data indicate them. Simulations and a real sepsis prediction study support the theory and illustrate when synthetic augmentation helps, when it cannot, and how to tune its quantity effectively.

1 Introduction

Imbalanced classification, where one class is observed far less frequently than the other, is a pervasive obstacle in modern statistical learning. Standard empirical risk minimization tends to favor overall accuracy, which often leads to systematically degraded detection of

*Department of Electrical & Computer Engineering, Duke University

†Department of Biostatistics & Bioinformatics and Department of Computer Science, Duke University

the minority class. This failure mode is especially consequential when the rare events are clinically, economically, or operationally important, as in medical data analysis (Salmi et al., 2024; Hung et al., 2022; Faviez et al., 2020), finance (Chen et al., 2024b; Tong and Shen, 2023; Subudhi and Panigrahi, 2018), and industrial anomaly detection (Bougaham et al., 2024; Piciarelli et al., 2021). These challenges motivate a renewed statistical focus on mitigating imbalance in a principled way, without turning augmentation into a purely heuristic step (Chen et al., 2024a).

A classic response to imbalance is to augment the minority class with additional (real or synthetic) samples, so that model training is less dominated by the majority class. The simplest mechanism is bootstrap-style oversampling, i.e., resampling minority observations with replacement (Efron and Tibshirani, 1994). A widely used alternative is SMOTE, which creates new minority examples by interpolating between a minority observation and its neighbors (Chawla et al., 2002). SMOTE has inspired many extensions, including ADASYN (He et al., 2008), Borderline-SMOTE (Han et al., 2005), safe-level-SMOTE (Bunkhumpornpat et al., 2009), and DBSMOTE (Bunkhumpornpat et al., 2012). Related augmentation strategies include Mixup (Zhang et al., 2017) and conditional data synthesis approaches (Tian and Shen, 2025). Beyond classical generators, modern deep generative models can also serve as synthetic sample generators, including VAEs (Kingma and Welling, 2013), normalizing flows (Papamakarios et al., 2021), GANs (Goodfellow et al., 2014), and diffusion/score-based models (Ho et al., 2020; Song et al., 2020). More recently, attention-based large language models have also been explored for synthetic data generation (Nakada et al., 2024). For a broad view of deep generative synthetic data across modalities and domains, see Eigenschink et al. (2023).

What remains unclear: when does augmentation help, and how much is enough? Despite the breadth of methods and applications, two basic questions remain surprisingly under-resolved from a statistical perspective.

First, *synthetic augmentation is not guaranteed to help*. Synthetic samples are generated from an estimated minority distribution. Augmentation can reduce the impact of imbalance, but it can simultaneously introduce distributional mismatch (because the generator is imperfect) and alter the effective variance of learning. As a result, the net effect on the target performance criterion can be positive or negative depending on data geometry and generator quality.

Second, *even when augmentation is beneficial, it is unclear how many synthetic samples should be added*. A common practice is *naive balancing*: generate enough synthetic minority samples so that the minority-plus-synthetic count matches the majority count. This rule is simple and often reasonable, but it is largely heuristic. Crucially, synthetic samples generally do not carry the same information content as independent real samples, and their mismatch can interact with the sample size in nontrivial ways.

Our perspective: treat augmentation as a controllable statistical operation. This paper develops a unified framework that treats synthetic augmentation as a *controllable* statistical operation and studies the risk trade-offs it induces. Our focus is the performance

under a *balanced* evaluation criterion (i.e., treating the two classes symmetrically at the population level), which is common in imbalanced learning when minority detection is a primary goal. Within this framework, augmentation is characterized by two ingredients: (1) the *synthetic size* (how many synthetic minority samples are added), and (2) the *generator mismatch* (how the synthetic minority distribution differs from the true minority distribution). Our analysis shows that these two factors jointly determine whether augmentation helps, how it helps, and when it can be harmful.

Two guiding questions and the regimes they reveal. We use our framework to answer two high-level questions that map directly to practice.

Q1. Does augmenting with synthetic samples always help in imbalanced learning?

Augmenting the minority class is often beneficial, but not universal. The key distinction is whether imbalance creates a *first-order* distortion of the learning objective near the population optimum under the balanced criterion. In many problems, the majority and minority contribute differently in the optimization-relevant directions; in this case, changing the effective class proportions can meaningfully shift the learned solution toward the balanced target. We refer to this as a *local asymmetry* regime, and it is precisely the setting in which synthetic augmentation can help.

However, our analysis also identifies an important regime where synthetic augmentation *cannot* help, even under severe imbalance. In this regime, the learning problem exhibits a form of “local symmetry”: near the balanced optimum, the two classes already exert equal first-order influence in the directions that matter for optimization. Then imbalance is not the bottleneck, and adding synthetic minority samples provides little benefit. Moreover, if the generator is imperfect, adding more synthetic samples can amplify mismatch effects and degrade performance. We develop this phenomenon in detail in Section 5.

Q2. Is naive balancing truly the best?

Naive balancing is not universally optimal, although it is often a sensible default. Whether it is optimal depends on generator quality and, more subtly, on whether the residual synthetic mismatch aligns with the intrinsic majority–minority difference in the learning problem. When the generator is consistent and there is no usable directional structure in its remaining mismatch, naive balancing is essentially rate-optimal: it corrects the leading imbalance effect, and finer tuning yields at most constant-factor improvements. In contrast, when the mismatch is directionally aligned with the majority–minority discrepancy, then a *small* adjustment around naive balancing can reduce the leading bias and yield a measurable improvement. Finally, for systematically biased (inconsistent) generators, tuning the synthetic size may be necessary for consistency, and the best choice can be far from naive balancing when bias cancellation is possible; when the mismatch direction is not aligned, adjusting the quantity alone cannot remove the bias.

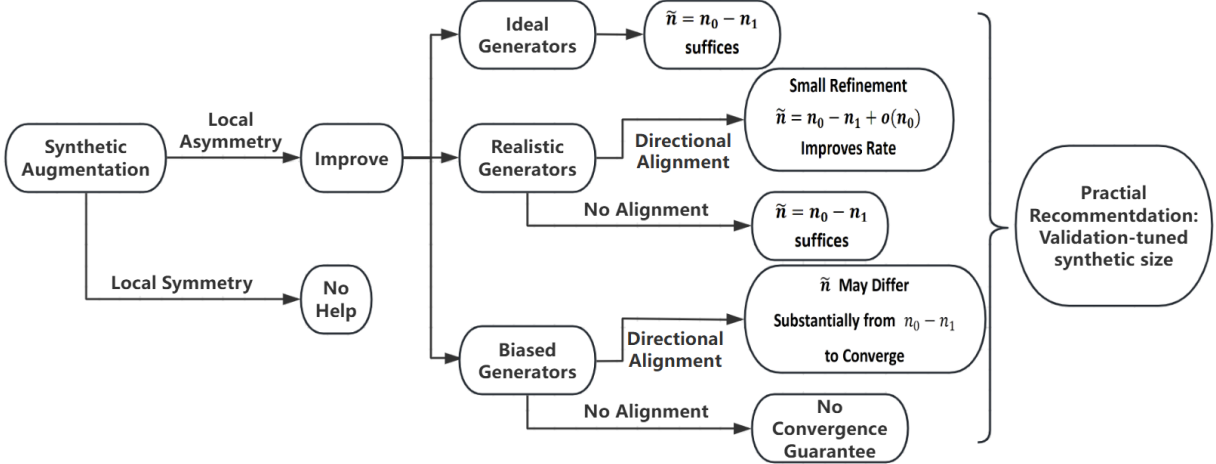


Figure 1: Flowchart of main results.

A practical recommendation: treat synthetic size as a tunable hyperparameter. In real applications, the relevant regime and mismatch direction are rarely known a priori. Motivated by the theory, we propose a simple and robust procedure, *Validation-Tuned Synthetic Size (VTSS)*: sweep a range of synthetic sizes (typically near naive balancing) and choose the value that minimizes balanced validation loss. VTSS is implementation-friendly, captures potential gains from nontrivial sizing, and automatically avoids harmful over-synthesis in regimes where synthetic data does not help.

The main messages of our theory are summarized in Figure 1, which maps the local asymmetry/symmetry regimes and generator quality to when synthetic augmentation helps and how the synthetic size should be chosen.

Related work. Synthetic minority augmentation has a long history in statistics and machine learning, including bootstrap-style oversampling (Efron and Tibshirani, 1994), SMOTE (Chawla et al., 2002) and its variants such as Borderline-SMOTE (Han et al., 2005), ADASYN (He et al., 2008), safe-level-SMOTE (Bunkhumpornpat et al., 2009), and DB-SMOTE (Bunkhumpornpat et al., 2012), as well as related augmentation strategies such as Mixup (Zhang et al., 2017) and conditional synthesis (Tian and Shen, 2025). Deep generative approaches include VAEs (Kingma and Welling, 2013), normalizing flows (Papamakarios et al., 2021), GANs (Goodfellow et al., 2014), and diffusion/score-based models (Ho et al., 2020; Song et al., 2020); LLM-based oversampling has also been studied (Nakada et al., 2024). A broader survey of deep generative approaches to synthetic data can be found in Eigenschink et al. (2023).

Recent theoretical work has begun to clarify statistical properties of learning with synthetic data. Nakada et al. (2024) provides theoretical guarantees for when LLM-generated minority samples can improve learning under imbalance and discusses interactions between generator quality and augmentation size. Lyu et al. (2025) emphasizes that naively treating synthetic samples as real can introduce systematic bias and proposes bias-correction strate-

gies with extensions beyond standard imbalanced classification. For uncertainty quantification and inference, Keret and Shojaie (2025) studies inference with AI-generated synthetic data for generalized linear models, while Räisä et al. (2025) develops a Bayesian framework that accounts for the synthetic generation mechanism and establishes conditions for consistent inference. Xia and Klusowski (2026) frames imbalanced classification as transfer learning under label shift and highlights settings in which oversampling incurs a cost, including curse-of-dimensionality effects for SMOTE. Ahmad et al. (2025) develops uniform concentration bounds comparing empirical risk on synthetic samples to the true minority risk and derives excess-risk guarantees for kernel-based classifiers.

A growing body of applied work illustrates synthetic augmentation in downstream analyses. In medical imaging, Ktena et al. (2024) uses conditional diffusion models for label-steerable augmentation and studies robustness and fairness under distribution shift. Rodriguez-Almeida et al. (2022) generates synthetic patient records for small, imbalanced disease prediction datasets, and Wang et al. (2025) studies self-improving generative foundation models for medical images and downstream gains from synthetic images. In finance, Roy et al. (2024) uses diffusion-generated transaction samples to augment scarce fraud cases. In time-series and industrial applications, Stanton et al. (2024) synthesizes time-series sensor datasets to support downstream predictive maintenance modeling.

Our work differs from these lines by providing a unified, risk-based characterization of when synthetic augmentation helps versus when it cannot, and by showing that the *choice of synthetic size* is a first-order practical decision rather than a fixed heuristic. Our theory isolates qualitative regimes (local asymmetry vs. local symmetry), explains the bias–variance trade-offs induced by generator mismatch and synthetic size, and motivates VTSS as a robust practical procedure.

Organization. The rest of this paper is organized as follows. Section 2 introduces the notation and formal setup for imbalanced classification with synthetic minority augmentation, and defines the balanced evaluation objective used throughout. Section 3 develops our main excess-risk characterization, which makes explicit how performance depends on both class-proportion imbalance and generator-induced distributional mismatch. Section 4 studies the local asymmetry regime in which synthetic augmentation can improve learning, and shows how the optimal synthetic size depends on generator quality and the directional structure of its bias. Section 5 identifies a local symmetry regime in which imbalance is not the dominant bottleneck, so synthetic augmentation cannot improve rates and may degrade performance when the generator is imperfect. Section 6 then presents our practical procedure, Validation-Tuned Synthetic Size (VTSS), which selects the synthetic size by minimizing balanced validation loss. Section 7 provides simulation studies that verify the qualitative predictions of the theory and evaluate VTSS. Section 8 concludes with discussion and future directions. Proofs and technical details are deferred to the supplementary materials.

2 Notation and Problem Formulation

Notation. For nonnegative sequences $\{a_n\}$ and $\{b_n\}$, we write $a_n \lesssim b_n$ (resp. $a_n \gtrsim b_n$) if there exists a universal constant $C > 0$ such that $a_n \leq Cb_n$ (resp. $a_n \geq Cb_n$). We write $a_n \asymp b_n$ if both $a_n \lesssim b_n$ and $b_n \lesssim a_n$ hold, and write $a_n \ll b_n$ (resp. $a_n \gg b_n$) if $a_n/b_n \rightarrow 0$ (resp. $a_n/b_n \rightarrow \infty$).

Vectors are denoted by boldface letters (e.g., $\mathbf{x}, \mathbf{y}, \mathbf{u}, \mathbf{v}$), and $\|\cdot\|$ denotes the Euclidean norm. Gradients and Hessians with respect to $\boldsymbol{\theta}$ are denoted by ∇ and ∇^2 . For two nonzero vectors \mathbf{u}, \mathbf{v} of the same dimension, we denote their angle and the sine value by

$$\angle(\mathbf{u}, \mathbf{v}) := \arccos\left(\frac{\mathbf{u}^\top \mathbf{v}}{\|\mathbf{u}\| \|\mathbf{v}\|}\right), \quad \sin \angle(\mathbf{u}, \mathbf{v}) = \sqrt{1 - \left(\frac{\mathbf{u}^\top \mathbf{v}}{\|\mathbf{u}\| \|\mathbf{v}\|}\right)^2}.$$

For a symmetric matrix A , let $\lambda_{\max}(A)$ and $\lambda_{\min}(A)$ denote its largest and smallest eigenvalues. For symmetric matrices A and B , we write $A \succeq B$ (resp. $A \succ B$) if $A - B$ is positive semidefinite (resp. positive definite).

Throughout, we work in an asymptotic regime where the data-generating distributions are fixed while the sample size grows. We use standard stochastic order notation $O_P(\cdot)$, $o_P(\cdot)$, $\Omega_P(\cdot)$, and $\Theta_P(\cdot)$. In particular, for sequences indexed by (n_0, n_1) , we write $x_{(n_0, n_1)} = O_P(a_{(n_0, n_1)})$ as $n_0, n_1 \rightarrow \infty$ if $x_{(n_0, n_1)}/a_{(n_0, n_1)}$ is stochastically bounded, and write $x_{(n_0, n_1)} = o_P(1)$ if $x_{(n_0, n_1)} \rightarrow 0$ in probability. We write $x_{(n_0, n_1)} = \Omega_P(a_{(n_0, n_1)})$ if $x_{(n_0, n_1)}/a_{(n_0, n_1)}$ is stochastically bounded away from zero, and $x_{(n_0, n_1)} = \Theta_P(a_{(n_0, n_1)})$ if both $O_P(\cdot)$ and $\Omega_P(\cdot)$ hold.

Problem formulation. We consider binary classification under class imbalance, where $y = 0$ denotes the majority class and $y = 1$ denotes the minority class. Let the class-conditional distributions be

$$\mathbf{x} \mid (y = 0) \sim \mathcal{P}_0, \quad \mathbf{x} \mid (y = 1) \sim \mathcal{P}_1.$$

We observe n_0 majority samples and n_1 minority samples, and we may augment the data with \tilde{n} synthetic minority samples. Synthetic covariates are drawn from a generator-induced distribution \mathcal{P}_{syn} ; since the generator is typically trained on the observed data, \mathcal{P}_{syn} may depend on (n_0, n_1) (more precisely, $\mathcal{P}_{\text{syn}, n_0, n_1}$), though we suppress this dependence for notational simplicity.

Let $\ell(\boldsymbol{\theta}; \mathbf{x}, y)$ be a loss function with parameter $\boldsymbol{\theta} \in \Theta$. Common choices include cross-entropy/logistic loss, squared loss, hinge loss, and exponential loss. To treat the two classes symmetrically at the population level, we define the **balanced population risk**

$$\mathcal{R}(\boldsymbol{\theta}) = \frac{1}{2} \mathbb{E}_{\mathcal{P}_0} \ell(\boldsymbol{\theta}; \mathbf{x}, 0) + \frac{1}{2} \mathbb{E}_{\mathcal{P}_1} \ell(\boldsymbol{\theta}; \mathbf{x}, 1), \quad (1)$$

and denote its minimizer by

$$\boldsymbol{\theta}^* = \arg \min_{\boldsymbol{\theta} \in \Theta} \mathcal{R}(\boldsymbol{\theta}).$$

Augmenting the training data with \tilde{n} synthetic minority samples changes the effective class proportions. Let

$$\pi_0 = \frac{n_0}{n_0 + n_1 + \tilde{n}}, \quad \pi_1 = \frac{n_1}{n_0 + n_1 + \tilde{n}}, \quad \tilde{\pi} = \frac{\tilde{n}}{n_0 + n_1 + \tilde{n}},$$

so that $\pi_0 + \pi_1 + \tilde{\pi} = 1$. The resulting **synthetic population risk** is

$$\tilde{\mathcal{R}}(\boldsymbol{\theta}) = \pi_0 \mathbb{E}_{\mathcal{P}_0} \ell(\boldsymbol{\theta}; \mathbf{x}, 0) + \pi_1 \mathbb{E}_{\mathcal{P}_1} \ell(\boldsymbol{\theta}; \mathbf{x}, 1) + \tilde{\pi} \mathbb{E}_{\mathcal{P}_{\text{syn}}} \ell(\boldsymbol{\theta}; \mathbf{x}, 1),$$

with minimizer $\hat{\boldsymbol{\theta}} = \arg \min_{\boldsymbol{\theta} \in \Theta} \tilde{\mathcal{R}}(\boldsymbol{\theta})$.

In practice, we observe $\{(\mathbf{x}_i, y_i)\}_{i=1}^{n_0+n_1}$ and generate synthetic samples

$$\{\tilde{\mathbf{x}}_i\}_{i=1}^{\tilde{n}} \sim \mathcal{P}_{\text{syn}}, \quad \tilde{y}_i \equiv 1.$$

We then minimize the **empirical augmented risk**

$$\begin{aligned} \hat{\mathcal{R}}(\boldsymbol{\theta}) &= \frac{1}{n_0 + n_1 + \tilde{n}} \left(\sum_{i=1}^{n_0+n_1} \ell(\boldsymbol{\theta}; \mathbf{x}_i, y_i) + \sum_{i=1}^{\tilde{n}} \ell(\boldsymbol{\theta}; \tilde{\mathbf{x}}_i, 1) \right) \\ &= \frac{1}{n_0 + n_1 + \tilde{n}} \left(\sum_{i=1}^{n_0} \ell(\boldsymbol{\theta}; \mathbf{x}_i^{(0)}, 0) + \sum_{i=1}^{n_1} \ell(\boldsymbol{\theta}; \mathbf{x}_i^{(1)}, 1) + \sum_{i=1}^{\tilde{n}} \ell(\boldsymbol{\theta}; \tilde{\mathbf{x}}_i, 1) \right), \end{aligned}$$

where $\{\mathbf{x}_i^{(0)}\}_{i=1}^{n_0}$ and $\{\mathbf{x}_i^{(1)}\}_{i=1}^{n_1}$ are the observed majority and minority samples. Let

$$\hat{\boldsymbol{\theta}} = \arg \min_{\boldsymbol{\theta} \in \Theta} \hat{\mathcal{R}}(\boldsymbol{\theta}).$$

Our goal is to estimate the balanced-risk optimizer $\boldsymbol{\theta}^*$ from imbalanced data, and to understand how synthetic augmentation, through \tilde{n} and \mathcal{P}_{syn} , affects the balanced excess risk $\mathcal{R}(\hat{\boldsymbol{\theta}}) - \mathcal{R}(\boldsymbol{\theta}^*)$.

3 Excess Risk Analysis for Imbalanced Classification

In this section, we establish a fundamental limitation on the balanced excess risk when training on imbalanced data augmented with synthetic minority samples. The key obstruction is a *distribution bias* induced by (i) the effective class weighting in the augmented training population, which typically differs from the target balanced design ($\pi_0 = 1/2$), and (ii) mismatch between the synthetic distribution \mathcal{P}_{syn} and the true minority distribution \mathcal{P}_1 . We begin by making these two effects explicit through a decomposition of the synthetic population risk, and then use it to characterize $\mathcal{R}(\hat{\boldsymbol{\theta}}) - \mathcal{R}(\boldsymbol{\theta}^*)$.

A key decomposition of the synthetic risk. Recall the balanced population risk $\mathcal{R}(\boldsymbol{\theta})$ and the synthetic population risk $\tilde{\mathcal{R}}(\boldsymbol{\theta})$. A direct calculation yields

$$\tilde{\mathcal{R}}(\boldsymbol{\theta}) = \mathcal{R}(\boldsymbol{\theta}) + \left(\pi_0 - \frac{1}{2}\right) \left[\mathbb{E}_{\mathcal{P}_0} \ell(\boldsymbol{\theta}; \mathbf{x}, 0) - \mathbb{E}_{\mathcal{P}_1} \ell(\boldsymbol{\theta}; \mathbf{x}, 1) \right] + \tilde{\pi} \left[\mathbb{E}_{\mathcal{P}_{\text{syn}}} \ell(\boldsymbol{\theta}; \mathbf{x}, 1) - \mathbb{E}_{\mathcal{P}_1} \ell(\boldsymbol{\theta}; \mathbf{x}, 1) \right]. \quad (2)$$

To streamline notation, define

$$\phi(\boldsymbol{\theta}) := \mathbb{E}_{\mathcal{P}_0} \ell(\boldsymbol{\theta}; \mathbf{x}, 0) - \mathbb{E}_{\mathcal{P}_1} \ell(\boldsymbol{\theta}; \mathbf{x}, 1), \quad (3)$$

$$\psi(\boldsymbol{\theta}) := \mathbb{E}_{\mathcal{P}_{\text{syn}}} \ell(\boldsymbol{\theta}; \mathbf{x}, 1) - \mathbb{E}_{\mathcal{P}_1} \ell(\boldsymbol{\theta}; \mathbf{x}, 1), \quad (4)$$

where $\phi(\boldsymbol{\theta})$ measures the local majority–minority asymmetry under the loss and $\psi(\boldsymbol{\theta})$ quantifies the synthetic-to-minority discrepancy. With these definitions, (2) becomes

$$\tilde{\mathcal{R}}(\boldsymbol{\theta}) = \mathcal{R}(\boldsymbol{\theta}) + \left(\pi_0 - \frac{1}{2}\right) \phi(\boldsymbol{\theta}) + \tilde{\pi} \psi(\boldsymbol{\theta}). \quad (5)$$

Here, $\left(\pi_0 - \frac{1}{2}\right) \phi(\boldsymbol{\theta}) + \tilde{\pi} \psi(\boldsymbol{\theta})$ is the *risk-level* distribution bias induced by class-proportion mismatch and generator mismatch. Since our excess-risk analysis is driven by first-order optimality conditions, we will work with the gradient of this bias term. Accordingly, we define the corresponding *first-order bias vector*

$$\mathbf{b}(\boldsymbol{\theta}) := \left(\pi_0 - \frac{1}{2}\right) \nabla \phi(\boldsymbol{\theta}) + \tilde{\pi} \nabla \psi(\boldsymbol{\theta}), \quad (6)$$

which is exactly the $\boldsymbol{\theta}$ -gradient of the bias component in (5).

A lower bound for balanced excess risk. The next result shows that, even asymptotically, the estimator trained on the augmented population can incur a non-vanishing balanced excess risk unless the induced bias is controlled.

Theorem 1 (Excess Risk Lower Bound). *Assume the parameter space is bounded, $\boldsymbol{\theta} \in \{\boldsymbol{\theta} : \|\boldsymbol{\theta}\| \leq B\}$. Suppose the covariates \mathbf{x} have bounded support and the loss $\ell(\boldsymbol{\theta}; \mathbf{x}, y)$ is continuous in $\boldsymbol{\theta}$ and bounded on bounded $(\boldsymbol{\theta}, \mathbf{x})$. Assume $\mathcal{R}(\boldsymbol{\theta})$ is continuous and $\tilde{\mathcal{R}}(\boldsymbol{\theta})$ admits a unique minimizer. Further suppose that $\nabla \tilde{\mathcal{R}}(\boldsymbol{\theta})$ is Lipschitz at its minimizer $\tilde{\boldsymbol{\theta}}$, i.e.,*

$$\|\nabla \tilde{\mathcal{R}}(\boldsymbol{\theta}) - \nabla \tilde{\mathcal{R}}(\tilde{\boldsymbol{\theta}})\| \leq M \|\boldsymbol{\theta} - \tilde{\boldsymbol{\theta}}\|,$$

and that $\mathcal{R}(\boldsymbol{\theta})$ is (locally) strongly convex at its minimizer $\boldsymbol{\theta}^*$:

$$\mathcal{R}(\boldsymbol{\theta}) \geq \mathcal{R}(\boldsymbol{\theta}^*) + \frac{\mu}{2} \|\boldsymbol{\theta} - \boldsymbol{\theta}^*\|^2.$$

Then the balanced excess risk satisfies

$$\mathcal{R}(\hat{\boldsymbol{\theta}}) - \mathcal{R}(\boldsymbol{\theta}^*) \geq \frac{\mu}{2M^2} \left\| \left(\pi_0 - \frac{1}{2}\right) \nabla \phi(\boldsymbol{\theta}^*) + \tilde{\pi} \nabla \psi(\boldsymbol{\theta}^*) \right\|^2 + o_P(1).$$

Theorem 1 shows that the leading lower bound is governed by the squared norm of the *first-order bias vector*

$$\mathbf{b}(\boldsymbol{\theta}^*) := (\pi_0 - \frac{1}{2}) \nabla \phi(\boldsymbol{\theta}^*) + \tilde{\pi} \nabla \psi(\boldsymbol{\theta}^*).$$

The term proportional to $\pi_0 - \frac{1}{2}$ reflects the class-proportion mismatch in the augmented population, whereas the term proportional to $\tilde{\pi}$ captures generator mismatch through $\mathcal{P}_{\text{syn}} - \mathcal{P}_1$. In particular, a necessary condition for balanced-risk consistency, i.e., $\mathcal{R}(\hat{\boldsymbol{\theta}}) - \mathcal{R}(\boldsymbol{\theta}^*) \rightarrow 0$, is $\|\mathbf{b}(\boldsymbol{\theta}^*)\| \rightarrow 0$.

Excess Risk Asymptotic Representation. We next state the conditions under which the excess risk admits an explicit asymptotic representation. These assumptions are standard regularity conditions in statistical learning theory and allow us to refine the lower bound in Theorem 1 into an exact decomposition in Theorem 2.

Assumption 1 (Condition for Excess Risk Asymptotic Representation).

(A1) *The balanced risk \mathcal{R} is differentiable and satisfies at its minimizer $\boldsymbol{\theta}^*$ for a constant $\mu > 0$ that*

$$\mathcal{R}(\boldsymbol{\theta}^*) \geq \mathcal{R}(\boldsymbol{\theta}) + \nabla \mathcal{R}(\boldsymbol{\theta})^\top (\boldsymbol{\theta}^* - \boldsymbol{\theta}) + \frac{\mu}{2} \|\boldsymbol{\theta}^* - \boldsymbol{\theta}\|^2;$$

(A2) *The population risk \mathcal{R} satisfies $\mathcal{R}(\boldsymbol{\theta}) - \mathcal{R}(\boldsymbol{\theta}^*) \geq L \|\boldsymbol{\theta} - \boldsymbol{\theta}^*\|^2$ at the minimizer $\boldsymbol{\theta}^*$ for some constant $L > 0$;*

(A3) *The covariates \mathbf{x} have bounded support and a finite third moment;*

(A4) *$\nabla^2 \tilde{\mathcal{R}}(\boldsymbol{\theta}) \succeq \lambda I$ for some $\lambda > 0$, and satisfies $\|\nabla^2 \tilde{\mathcal{R}}(\boldsymbol{\theta}) - \nabla^2 \tilde{\mathcal{R}}(\tilde{\boldsymbol{\theta}})\| \leq L \|\boldsymbol{\theta} - \tilde{\boldsymbol{\theta}}\|$ at the minimizer $\tilde{\boldsymbol{\theta}}$ for a constant $L > 0$;*

(A5) *$\Sigma_0(\tilde{\boldsymbol{\theta}}), \Sigma_1(\tilde{\boldsymbol{\theta}}), \tilde{\Sigma}(\tilde{\boldsymbol{\theta}}) \succ \lambda I$ for some $\lambda > 0$, have finite largest eigenvalue. $\Sigma(\boldsymbol{\theta})$ satisfies $\|\Sigma(\tilde{\boldsymbol{\theta}}) - \Sigma(\boldsymbol{\theta}^*)\| \leq L \|\tilde{\boldsymbol{\theta}} - \boldsymbol{\theta}^*\|$ at two minimizers $\tilde{\boldsymbol{\theta}}$ and $\boldsymbol{\theta}^*$ for a constant $L > 0$;*

(A6) *A finite gradient of total bias:*

$$\|(\pi_0 - 1/2) \nabla^2 \phi(\boldsymbol{\theta}) + \tilde{\pi} \nabla^2 \psi(\boldsymbol{\theta})\| \leq C < \infty.$$

Theorem 2 (Excess Risk Decomposition). *Define the covariance matrices of the loss gradients:*

$$\begin{aligned} \Sigma_0(\boldsymbol{\theta}) &= \text{Cov}_{\mathcal{P}_0}(\nabla_{\boldsymbol{\theta}} \ell(\boldsymbol{\theta}; \mathbf{x}, 0)), & \Sigma_1(\boldsymbol{\theta}) &= \text{Cov}_{\mathcal{P}_1}(\nabla_{\boldsymbol{\theta}} \ell(\boldsymbol{\theta}; \mathbf{x}, 1)), \\ \tilde{\Sigma}(\boldsymbol{\theta}) &= \text{Cov}_{\mathcal{P}_{\text{syn}}}(\nabla_{\boldsymbol{\theta}} \ell(\boldsymbol{\theta}; \mathbf{x}, 1)), & \Sigma(\boldsymbol{\theta}) &:= \frac{n_0 \Sigma_0(\boldsymbol{\theta}) + n_1 \Sigma_1(\boldsymbol{\theta}) + \tilde{n} \tilde{\Sigma}(\boldsymbol{\theta})}{n_0 + n_1 + \tilde{n}}. \end{aligned} \quad (7)$$

Suppose Assumption 1 holds. For large enough n_0 and n_1 , there exists a random vector $Z \sim \mathcal{N}(0, I_d)$ such that

$$\begin{aligned} & \mathcal{R}(\hat{\boldsymbol{\theta}}) - \mathcal{R}(\boldsymbol{\theta}^*) \\ &= \frac{1}{2} \mathbf{b}(\boldsymbol{\theta}^*)^\top [\nabla^2 \mathcal{R}(\boldsymbol{\theta}^*) + \nabla \mathbf{b}(\boldsymbol{\theta}^*)]^{-1} \nabla^2 \mathcal{R}(\boldsymbol{\theta}^*) [\nabla^2 \mathcal{R}(\boldsymbol{\theta}^*) + \nabla \mathbf{b}(\boldsymbol{\theta}^*)]^{-1} \mathbf{b}(\boldsymbol{\theta}^*) \\ &\quad - \frac{1}{\sqrt{n_0 + n_1 + \tilde{n}}} \mathbf{b}(\boldsymbol{\theta}^*)^\top [\nabla^2 \mathcal{R}(\boldsymbol{\theta}^*) + \nabla \mathbf{b}(\boldsymbol{\theta}^*)]^{-1} \nabla^2 \mathcal{R}(\boldsymbol{\theta}^*) [\nabla^2 \mathcal{R}(\boldsymbol{\theta}^*) + \nabla \mathbf{b}(\boldsymbol{\theta}^*)]^{-1} \Sigma(\boldsymbol{\theta}^*)^{\frac{1}{2}} Z \\ &\quad + \frac{1}{2(n_0 + n_1 + \tilde{n})} Z^\top \Sigma(\boldsymbol{\theta}^*)^{\frac{1}{2}} [\nabla^2 \mathcal{R}(\boldsymbol{\theta}^*) + \nabla \mathbf{b}(\boldsymbol{\theta}^*)]^{-1} \nabla^2 \mathcal{R}(\boldsymbol{\theta}^*) [\nabla^2 \mathcal{R}(\boldsymbol{\theta}^*) + \nabla \mathbf{b}(\boldsymbol{\theta}^*)]^{-1} \Sigma(\boldsymbol{\theta}^*)^{\frac{1}{2}} Z + R. \end{aligned}$$

Here $\mathbf{b}(\boldsymbol{\theta}) = (\pi_0 - \frac{1}{2}) \nabla \phi(\boldsymbol{\theta}) + \tilde{\pi} \nabla \psi(\boldsymbol{\theta})$, so $\nabla \mathbf{b}(\boldsymbol{\theta}) = (\pi_0 - \frac{1}{2}) \nabla^2 \phi(\boldsymbol{\theta}) + \tilde{\pi} \nabla^2 \psi(\boldsymbol{\theta})$ denotes the Jacobian. The remainder term R satisfies

$$R = O_P \left(\|\mathbf{b}(\boldsymbol{\theta}^*)\|^3 + (n_0 + n_1 + \tilde{n})^{-3/2} + \frac{1}{n_0 + n_1 + \tilde{n}} \|\mathbf{b}(\boldsymbol{\theta}^*)\| + \frac{1}{\sqrt{n_0 + n_1 + \tilde{n}}} \|\mathbf{b}(\boldsymbol{\theta}^*)\|^2 \right).$$

Theorem 2 expresses the excess risk as the sum of three leading terms and a higher-order remainder. The first term is a quadratic form in $\mathbf{b}(\boldsymbol{\theta}^*)$ and captures the deterministic *distribution bias* induced by the effective weights $(\pi_0, \pi_1, \tilde{\pi})$ and any discrepancy between \mathcal{P}_{syn} and \mathcal{P}_1 . The second and third terms quantify stochastic fluctuations through the covariance $\Sigma(\boldsymbol{\theta}^*)$ and the Gaussian limit Z , thereby making the bias–variance trade-off explicit as a function of (n_0, n_1, \tilde{n}) . This representation is useful in two ways. First, since the right-hand side depends on \tilde{n} through $\mathbf{b}(\boldsymbol{\theta}^*)$, $\nabla \mathbf{b}(\boldsymbol{\theta}^*)$, and $\Sigma(\boldsymbol{\theta}^*)$, it can be minimized with respect to \tilde{n} to obtain principled synthetic-size choices. Second, different generators affect the expansion only through $\psi(\boldsymbol{\theta})$ and $\tilde{\Sigma}(\boldsymbol{\theta})$, providing a common asymptotic scale for comparing generators: holding (n_0, n_1, \tilde{n}) fixed, generators are preferable when they yield smaller bias $\mathbf{b}(\boldsymbol{\theta}^*)$ and/or more favorable covariance contributions.

Remark 1 (User-specific class weights). *Our presentation focuses on the balanced objective ($\rho = \frac{1}{2}$) for clarity, but all results extend directly to user-specified class weights. Fix $\rho \in (0, 1)$ as the weight on the majority class and define*

$$\mathcal{R}^\rho(\boldsymbol{\theta}) = \rho \mathbb{E}_{\mathcal{P}_0} \ell(\boldsymbol{\theta}; \mathbf{x}, 0) + (1 - \rho) \mathbb{E}_{\mathcal{P}_1} \ell(\boldsymbol{\theta}; \mathbf{x}, 1).$$

Then the synthetic population risk admits the decomposition

$$\tilde{\mathcal{R}}(\boldsymbol{\theta}) = \mathcal{R}^\rho(\boldsymbol{\theta}) + (\pi_0 - \rho) \phi(\boldsymbol{\theta}) + \tilde{\pi} \psi(\boldsymbol{\theta}),$$

so the corresponding first-order bias vector becomes

$$\mathbf{b}_\rho(\boldsymbol{\theta}) := (\pi_0 - \rho) \nabla \phi(\boldsymbol{\theta}) + \tilde{\pi} \nabla \psi(\boldsymbol{\theta}).$$

Consequently, Theorems 1 and 2 hold verbatim after replacing $\mathbf{b}(\boldsymbol{\theta})$ by $\mathbf{b}_\rho(\boldsymbol{\theta})$ (and replacing $\frac{1}{2}$ by ρ wherever it appears). Moreover, consistency under the ρ -weighted objective requires matching the target proportion $\pi_0 \rightarrow \rho$, i.e.,

$$\tilde{n} = \frac{1-\rho}{\rho} n_0 - n_1 + o(n_0),$$

and, as in the $\rho = \frac{1}{2}$ case, lower-order deviations of \tilde{n} around this target can affect rates.

In the remainder of this paper, we distinguish two regimes described as follows.

- **Local asymmetry:** $\|\nabla\phi(\boldsymbol{\theta}^*)\| \geq c$ for a fixed constant $c > 0$. In this case, synthetic minority augmentation may improve performance. In this regime, both generator quality (through $\|\nabla\psi(\boldsymbol{\theta}^*)\|$) and synthetic size \tilde{n} matter: too few synthetic samples may not sufficiently mitigate imbalance, while too many may amplify generator-induced bias.
- **Local symmetry:** $\|\nabla\phi(\boldsymbol{\theta}^*)\| = 0$. In this case, synthetic minority samples typically do not help and may degrade performance.

4 Local Asymmetry: When Synthetic Minority Samples May Improve Performance

We now focus on the locally asymmetric regime, where $\|\nabla\phi(\boldsymbol{\theta}^*)\| \geq c > 0$. Here the choice of synthetic sample size \tilde{n} interacts with the generator mismatch $\|\nabla\psi(\boldsymbol{\theta}^*)\|$, leading to a bias–variance trade-off that determines whether augmentation improves or harms performance. Accordingly, we organize the analysis by generator quality, considering the following three regimes in Sections 4.1, 4.2, and 4.3, respectively.

1. **Ideal synthetic minority-class sample generator:** $\|\nabla\psi(\boldsymbol{\theta}^*)\| \ll n_0^{-1/2}$. This regime primarily serves as a theoretical benchmark. If the generator is trained using only the available minority data, then even under favorable conditions that avoid the curse of dimensionality (as is often assumed in nonparametric settings), the estimation error of the learned minority distribution is fundamentally limited by the sample size n_1 , yielding at best a parametric-rate scaling of $n_1^{-1/2}$. More broadly, even when the majority and minority distributions share exploitable structure and the generator can, in principle, leverage information from both classes, the best achievable accuracy is still bounded by parametric scaling with the total sample size, namely $(n_0+n_1)^{-1/2} \asymp n_0^{-1/2}$ in the imbalanced regime. Consequently, requiring $\|\nabla\psi(\boldsymbol{\theta}^*)\| \ll n_0^{-1/2}$ is generally unattainable for standard, data-trained generators.
2. **Realistic synthetic minority-class sample generator:** $n_0^{-1/2} \ll \|\nabla\psi(\boldsymbol{\theta}^*)\| \ll 1$. This corresponds to the practically relevant case, where the residual synthetic mismatch is non-negligible yet bounded.
3. **Inconsistent synthetic minority-class sample generator:** $\|\nabla\psi(\boldsymbol{\theta}^*)\| \gtrsim 1$.

The thresholds separating the ideal, realistic, and inconsistent regimes are well motivated: for standard data-trained generators, residual mismatch is typically limited by parametric-order scaling with the available sample size, making $\|\nabla\psi(\boldsymbol{\theta}^*)\| \ll n_0^{-1/2}$ unrealistic. At the other extreme, a mismatch bounded away from zero (i.e., $\|\nabla\psi(\boldsymbol{\theta}^*)\| \gtrsim 1$) indicates persistent distributional error and may compromise consistency. Nevertheless, the ideal and inconsistent regimes provide useful benchmarks for isolating algorithmic and statistical behavior.

4.1 With Ideal Synthetic Sample Generators

We first study the regime of *ideal* synthetic generators, where the synthetic distribution \mathcal{P}_{syn} closely matches the true minority distribution \mathcal{P}_1 . Intuitively, when the generator-induced mismatch is negligible, the precise choice of the synthetic sample size \tilde{n} should matter only weakly: as long as \tilde{n} is chosen at the appropriate order of $n_0 - n_1$ (so that the effective class proportions are approximately balanced), the estimator based on synthetic augmentation should perform well.

The next theorem formalizes this intuition. It shows that, under an ideal generator, any synthetic size \tilde{n} that stays sufficiently close to the balancing choice $\tilde{n} = n_0 - n_1$ yields the same $1/n_0$ convergence rate. In this regime, tuning \tilde{n} can at best improve constant factors, but cannot improve the rate.

Theorem 3 (Excess risk under an ideal synthetic generator). *Assume the conditions of Theorem 2. Suppose moreover that the curvature contribution from the synthetic mismatch is controlled in the sense that*

$$\|\nabla^2\psi(\boldsymbol{\theta}^*)\| \leq \lambda_{\min}(\nabla^2\mathcal{R}(\boldsymbol{\theta}^*)).$$

If the generator is ideal, satisfying $\|\nabla\psi(\boldsymbol{\theta}^)\| \ll n_0^{-1/2}$, then for any synthetic size*

$$\tilde{n} \in \mathcal{C} := \{\tilde{n} : \tilde{n} = n_0 - n_1 + o(\sqrt{n_0})\},$$

we have,

$$\mathcal{R}(\hat{\boldsymbol{\theta}}) - \mathcal{R}(\boldsymbol{\theta}^*) = \Theta_P(n_0^{-1}).$$

The set \mathcal{C} requires the effective class proportions to be balanced around 1/2 up to the natural $n_0^{-1/2}$ scale of stochastic fluctuations. Under an ideal generator, the leading bias term in Theorem 2 is dominated by the stochastic term as long as $\tilde{n} \in \mathcal{C}$, and the excess risk attains the classical balanced parametric rate $\mathcal{R}(\hat{\boldsymbol{\theta}}) - \mathcal{R}(\boldsymbol{\theta}^*) = \Theta_P(n_0^{-1})$. In particular, the naive balancing choice $\tilde{n} = n_0 - n_1$ already achieves the optimal rate. Adjusting \tilde{n} within \mathcal{C} may improve constants, but cannot surpass the n_0^{-1} rate.

4.2 With Realistic Synthetic Sample Generators

We next consider a more realistic regime in which the synthetic generator is statistically consistent, but its residual mismatch decays more slowly than the parametric rate:

$$n_0^{-1/2} \ll \|\nabla\psi(\boldsymbol{\theta}^*)\| \ll 1.$$

Our goal is to understand how the interaction between the intrinsic majority–minority imbalance and the generator-induced bias determines the appropriate order of the synthetic sample size \tilde{n} . To build intuition, we consider the following toy example.

Example 1 (Toy collinear case). Assume the generator is consistent with $\|\nabla\psi(\boldsymbol{\theta}^*)\| \asymp (\log n_1)^{-1/2}$, so $\|\nabla\psi(\boldsymbol{\theta}^*)\| \gg n_0^{-1/2}$. Write the leading terms in Theorem 2 as

$$\mathcal{R}(\hat{\boldsymbol{\theta}}) - \mathcal{R}(\boldsymbol{\theta}^*) = T_1 + T_2 + T_3 + R,$$

where $T_1 \asymp \|\mathbf{b}(\boldsymbol{\theta}^*)\|^2$, $T_2 = \Theta_P(n^{-1/2}\|\mathbf{b}(\boldsymbol{\theta}^*)\|)$, and $T_3 = \Theta_P(n^{-1})$, with $n = n_0 + n_1 + \tilde{n}$.

Since consistency requires $\tilde{n} \approx n_0 - n_1$, let $\tilde{n} = (n_0 - n_1)(1 + \delta_n)$ with $\delta_n \rightarrow 0$. If $\nabla\psi(\boldsymbol{\theta}^*)$ is collinear with $\nabla\phi(\boldsymbol{\theta}^*)$, i.e., $\nabla\psi(\boldsymbol{\theta}^*) = s(\log n_1)^{-1/2}\nabla\phi(\boldsymbol{\theta}^*)$ for $s \in \{\pm 1\}$, then one can choose $\delta_n = \Theta((\log n_1)^{-1/2})$ so that $\mathbf{b}(\boldsymbol{\theta}^*) = 0$. Consequently, $T_1 = T_2 = 0$ and $\mathcal{R}(\hat{\boldsymbol{\theta}}) - \mathcal{R}(\boldsymbol{\theta}^*) = \Theta_P(n_0^{-1})$.

In contrast, the naive balancing choice $\tilde{n} = n_0 - n_1$ leaves $\|\mathbf{b}(\boldsymbol{\theta}^*)\| = \Theta((\log n_1)^{-1/2})$, yielding a slower rate $\mathcal{R}(\hat{\boldsymbol{\theta}}) - \mathcal{R}(\boldsymbol{\theta}^*) = \Theta_P((\log n_1)^{-1})$.

Example 1 highlights two points. First, while $\tilde{n} \approx n_0 - n_1$ is necessary for consistency, the lower-order refinement of \tilde{n} around $n_0 - n_1$ can change the convergence rate. Second, the relative direction of $\nabla\psi(\boldsymbol{\theta}^*)$ and $\nabla\phi(\boldsymbol{\theta}^*)$ matters: alignment can either amplify or cancel the leading bias term $\mathbf{b}(\boldsymbol{\theta}^*)$. We next formalize these insights in a general setting.

Theorem 4 (Excess risk under a realistic synthetic generator). Suppose the assumptions of Theorem 2 hold and $\|\nabla^2\psi(\boldsymbol{\theta}^*)\| < \infty$. Assume the generator is realistic in the sense that $\|\nabla\psi(\boldsymbol{\theta}^*)\| \gg n_0^{-1/2}$, and that the alignment condition

$$\sin \angle(\nabla\phi(\boldsymbol{\theta}^*), \nabla\psi(\boldsymbol{\theta}^*)) \lesssim \frac{1}{\|\nabla\psi(\boldsymbol{\theta}^*)\| \sqrt{n_0}}$$

holds. Then:

- If we choose

$$\tilde{n} = \frac{n_0 - n_1 + O_P(\sqrt{n_0})}{1 - 2\|\nabla\psi(\boldsymbol{\theta}^*)\|/\|\nabla\phi(\boldsymbol{\theta}^*)\| + O_P(1/\sqrt{n_0})},$$

then $\mathcal{R}(\hat{\boldsymbol{\theta}}) - \mathcal{R}(\boldsymbol{\theta}^*) = \Theta_P(n_0^{-1})$.

- If we choose the naive balancing rule $\tilde{n} = n_0 - n_1$, then $\mathcal{R}(\hat{\boldsymbol{\theta}}) - \mathcal{R}(\boldsymbol{\theta}^*) = \Theta_P(\|\nabla\psi(\boldsymbol{\theta}^*)\|^2) \gg \Theta_P(n_0^{-1})$.

Theorem 4 formalizes a bias-cancellation phenomenon. When the generator mismatch $\nabla\psi(\boldsymbol{\theta}^*)$ is sufficiently aligned with the intrinsic shift $\nabla\phi(\boldsymbol{\theta}^*)$, a small refinement of \tilde{n} around $n_0 - n_1$ cancels the leading distribution bias and restores the parametric rate $\Theta_P(n_0^{-1})$. In contrast, the naive balancing rule $\tilde{n} = n_0 - n_1$ leaves a residual bias of order $\|\nabla\psi(\boldsymbol{\theta}^*)\|$, resulting in a slower excess-risk rate.

Practically, the result suggests treating \tilde{n} as a tuning parameter rather than a fixed balancing heuristic: useful directional information between $\nabla\phi(\boldsymbol{\theta}^*)$ and $\nabla\psi(\boldsymbol{\theta}^*)$ can guide a choice of \tilde{n} that reduces generator-induced bias and improve the performance.

4.3 With Inconsistent Synthetic Sample Generators

In this subsection, we aim to study the inconsistent regime as a robustness and failure-mode analysis. In practice, generators may be misspecified, capacity-limited, or trained with insufficient data, leading to a non-vanishing distributional mismatch even asymptotically. In this case, we consider the setting in which the mismatch does not vanish, e.g.,

$$\liminf_{n_0, n_1 \rightarrow \infty} \|\nabla \psi(\boldsymbol{\theta}^*)\| \gtrsim 1,$$

where $\psi(\cdot)$ is defined in equation (4). This implies that the total synthetic bias term $\mathbf{b}(\boldsymbol{\theta}^*)$ defined in Theorem 2 generally need not converge to zero, so the estimator may retain a non-vanishing bias unless additional directional structure between $\nabla \phi(\boldsymbol{\theta}^*)$ and $\nabla \psi(\boldsymbol{\theta}^*)$ is available and the synthetic size \tilde{n} is tuned accordingly.

The next theorem shows that (a) if $\mathbf{b}(\boldsymbol{\theta}^*)$ remains bounded away from zero, then the excess risk cannot converge to zero; (b) when $\nabla \phi(\boldsymbol{\theta}^*)$ and $\nabla \psi(\boldsymbol{\theta}^*)$ are approximately aligned, an appropriate choice of \tilde{n} can partially offset the persistent mismatch and restore consistency of the excess risk.

Theorem 5 (Excess risk under an inconsistent synthetic generator). *Suppose the synthetic bias satisfies $\liminf_{n_0, n_1 \rightarrow \infty} \|\nabla \psi(\boldsymbol{\theta}^*)\| \geq c$ for constant $c > 0$.*

- When synthetic direction is well aligned s.t. $\sin \angle(\nabla \phi(\boldsymbol{\theta}^*), \nabla \psi(\boldsymbol{\theta}^*)) = o_P(1)$, by selecting synthetic size

$$\tilde{n} = \frac{n_0 - n_1 + (n_0 + n_1)o(1)}{1 - 2\|\nabla \psi(\boldsymbol{\theta}^*)\|/\|\nabla \phi(\boldsymbol{\theta}^*)\| + o(1)},$$

the excess risk satisfies

$$\mathcal{R}(\hat{\boldsymbol{\theta}}) - \mathcal{R}(\boldsymbol{\theta}^*) = o_P(1).$$

- If either (i) the generator mismatch is not asymptotically aligned with the intrinsic shift, in the sense that there exists $c_0 > 0$ such that $\sin \angle(\nabla \phi(\boldsymbol{\theta}^*), \nabla \psi(\boldsymbol{\theta}^*)) > c_0 > 0$ in probability and $\tilde{n}/n_0 \rightarrow \rho$ for some $\rho \geq 0$, or (ii) the directions are aligned but we nevertheless choose the naive balancing rule $\tilde{n} = n_0 - n_1$, then there exists $c_1 > 0$ such that

$$\mathcal{R}(\hat{\boldsymbol{\theta}}) - \mathcal{R}(\boldsymbol{\theta}^*) \geq c_1 + o_P(1),$$

in probability.

Next, we provide two examples that illustrate the phenomena characterized by Theorem 5.

Example 2 (Two-dimensional Gaussian model). *Let $d = 2$. Suppose*

$$\mathbf{x} \mid y = 0 \sim \mathcal{P}_0 = \mathcal{N}(\mathbf{0}, I_2), \quad \mathbf{x} \mid y = 1 \sim \mathcal{P}_1 = \mathcal{N}(\boldsymbol{\mu}_1, I_2),$$

and synthetic minority samples are generated from $\tilde{\mathbf{x}} \sim \mathcal{P}_{\text{syn}} = \mathcal{N}(\boldsymbol{\mu}_s, I_2)$. We consider the squared loss $\ell(\boldsymbol{\theta}; \mathbf{x}, y) = (\boldsymbol{\theta}^\top \mathbf{x} - y)^2$.

(i) Aligned bias directions. Take $\boldsymbol{\mu}_1 = (\mu, 0)^\top$ and $\boldsymbol{\mu}_s = (a, 0)^\top$ with $a \notin \{\mu, 2/\mu\}$ to avoid degeneracy. In this case, $\nabla\phi(\boldsymbol{\theta}^*)$ and $\nabla\psi(\boldsymbol{\theta}^*)$ are collinear. Consequently, there exists a choice of synthetic sample size,

$$\tilde{n} = \frac{\mu(n_0 - n_1)}{a(\mu^2 + 2) - \mu(a^2 + 1)},$$

for which the leading bias cancels and the balanced excess risk satisfies

$$\mathcal{R}(\hat{\boldsymbol{\theta}}) - \mathcal{R}(\boldsymbol{\theta}^*) = O_P((n_0 + n_1 + \tilde{n})^{-1}).$$

However, the naive ‘‘balancing’’ choice $\tilde{n} = n_0 - n_1$ need not be sufficient for consistency. For example, when $\mu = 1$ and $a = \frac{1}{2}$, the bias-cancelling choice equals $\tilde{n} = 4(n_0 - n_1)$, whereas using $\tilde{n} = n_0 - n_1$ yields

$$\mathcal{R}(\hat{\boldsymbol{\theta}}) - \mathcal{R}(\boldsymbol{\theta}^*) \rightarrow c > 0 \quad \text{in probability.}$$

(ii) Orthogonal bias directions. Take $\boldsymbol{\mu}_1 = (\mu, 0)^\top$ and $\boldsymbol{\mu}_s = (\mu, \mu)^\top$ with $\mu^2 \leq 2$. Then $\nabla\phi(\boldsymbol{\theta}^*)$ and $\nabla\psi(\boldsymbol{\theta}^*)$ are orthogonal. In particular, if the synthetic fraction does not vanish (i.e., $\liminf \tilde{\pi} \geq \tau > 0$), the balanced excess risk remains bounded away from zero:

$$\mathcal{R}(\hat{\boldsymbol{\theta}}) - \mathcal{R}(\boldsymbol{\theta}^*) \rightarrow c > 0 \quad \text{in probability.}$$

Thus, when the synthetic mismatch introduces a bias component orthogonal to $\nabla\phi(\boldsymbol{\theta}^*)$, tuning \tilde{n} cannot eliminate the leading bias and consistency fails whenever synthetic augmentation has non-negligible weight.

5 Local Symmetry: When Synthetic Minority Samples May Degrade Performance

Synthetic minority augmentation is often motivated as a remedy for class imbalance: by increasing the frequency of minority-class samples, it can strengthen the learning signal for the minority and improve estimation and downstream performance. However, there is an important regime in which augmentation cannot help, and may even hurt, despite severe imbalance. The key phenomenon is a form of *local symmetry* at the balanced-risk minimizer, under which the two classes already contribute equally along the optimization-relevant directions. In such cases, imbalance is not the bottleneck, and any additional synthetic samples can only introduce distributional bias if the generator is imperfect.

Recall we say the problem exhibits *local symmetry* at $\boldsymbol{\theta}^*$ if

$$\nabla\phi(\boldsymbol{\theta}^*) = \nabla_{\boldsymbol{\theta}} \left\{ \mathbb{E}_{\mathcal{P}_0} \ell(\boldsymbol{\theta}; \mathbf{x}, 0) - \mathbb{E}_{\mathcal{P}_1} \ell(\boldsymbol{\theta}; \mathbf{x}, 1) \right\} \Big|_{\boldsymbol{\theta}=\boldsymbol{\theta}^*} = 0. \quad (8)$$

Condition (8) means that, at the balanced-risk optimum, the (population) gradient contributions from the majority and minority classes coincide; hence reweighting the classes provides

little first-order benefit near $\boldsymbol{\theta}^*$. In this regime, the leading bias term that governs the excess risk reduces to the generator-mismatch component. Specifically, writing the (vector) bias as

$$\mathbf{b}(\boldsymbol{\theta}^*) := \left(\pi_0 - \frac{1}{2} \right) \nabla \phi(\boldsymbol{\theta}^*) + \tilde{\pi} \nabla \psi(\boldsymbol{\theta}^*),$$

local symmetry implies $\mathbf{b}(\boldsymbol{\theta}^*) = \tilde{\pi} \nabla \psi(\boldsymbol{\theta}^*)$. Thus, setting $\tilde{\pi} = 0$ eliminates the synthetic component entirely, whereas adding many synthetic samples can amplify the mismatch bias through $\tilde{\pi}$. The next theorem quantifies this trade-off under a *realistic* generator that is imperfect but improving with sample size.

Theorem 6 (Realistic synthetic augmentation can degrade performance). *Under the assumptions of Theorem 2, suppose the local symmetry condition (8) holds and the synthetic generator is realistic in the sense that*

$$n_0^{-1/2} \ll \|\nabla \psi(\boldsymbol{\theta}^*)\| \ll 1.$$

Then the following hold:

- (**Diminishing synthetic size**). *If $\tilde{n} = O(\sqrt{n_0}/\|\nabla \psi(\boldsymbol{\theta}^*)\|) \ll n_0$, then*

$$\mathcal{R}(\hat{\boldsymbol{\theta}}) - \mathcal{R}(\boldsymbol{\theta}^*) = O_P(n_0^{-1}).$$

- (**Non-diminishing synthetic size**). *If $\tilde{n} \gtrsim n_0$, then*

$$\mathcal{R}(\hat{\boldsymbol{\theta}}) - \mathcal{R}(\boldsymbol{\theta}^*) = \Omega_P(\|\nabla \psi(\boldsymbol{\theta}^*)\|^2) \gg \Theta_P(n_0^{-1}).$$

Theorem 6 shows that, under local symmetry, synthetic augmentation cannot improve the balanced excess risk when the generator mismatch is non-negligible. If the synthetic size is diminishing, the estimator already achieves the baseline $O_P(n_0^{-1})$ rate, indicating that little or no augmentation is sufficient. In contrast, if the synthetic size is non-diminishing (of order n_0 or larger), the mismatch bias accumulates and the excess risk scales at least as $\|\nabla \psi(\boldsymbol{\theta}^*)\|^2$, which dominates the baseline n_0^{-1} rate. Intuitively, because the two classes already exert equal first-order influence near $\boldsymbol{\theta}^*$, adding synthetic minority samples provides no imbalance-related benefit and can only degrade performance by injecting distributional bias.

We next present two examples that satisfy the local symmetry condition (8). Section 7 further corroborates the theory via simulation.

Example 3 (Mean-shift model). *Consider a mean-shift model with $\Pr(y = 1) = \pi$ and $\Pr(y = 0) = 1 - \pi$, and class-conditionals*

$$\mathbf{x} | (y = 1) \sim \boldsymbol{\mu} + \boldsymbol{\xi}, \quad \mathbf{x} | (y = 0) \sim -\boldsymbol{\mu} + \boldsymbol{\xi},$$

where $\boldsymbol{\mu} \in \mathbb{R}^d$ is fixed and $\boldsymbol{\xi} \in \mathbb{R}^d$ has mean zero, bounded support, and full-rank covariance. Under the linear score $f_{\boldsymbol{\theta}}(\mathbf{x}) = \boldsymbol{\theta}^\top \mathbf{x}$ and squared loss $\ell(\boldsymbol{\theta}; \mathbf{x}, y) = (y - \frac{1}{2} - \boldsymbol{\theta}^\top \mathbf{x})^2$, the local symmetry condition (8) holds, i.e., $\nabla \phi(\boldsymbol{\theta}^*) = \mathbf{0}$.

Example 4 (Sigmoid Bernoulli logistic regression). Consider the sigmoid Bernoulli model (without intercept) with $\mathbf{x} \sim p(\mathbf{x})$ and

$$\Pr(y = 1 \mid \mathbf{x}) = \sigma(\mathbf{x}^\top \boldsymbol{\theta}_{\text{true}}), \quad \Pr(y = 0 \mid \mathbf{x}) = 1 - \sigma(\mathbf{x}^\top \boldsymbol{\theta}_{\text{true}}),$$

and logistic loss $\ell(\boldsymbol{\theta}; \mathbf{x}, y) = \log(1 + \exp\{\boldsymbol{\theta}^\top \mathbf{x}\}) - y\mathbf{x}^\top \boldsymbol{\theta}$. If

$$\mathbb{E}_{p(\mathbf{x})} \left[\mathbf{x} \sigma(\boldsymbol{\theta}_{\text{true}}^\top \mathbf{x}) (1 - \sigma(\boldsymbol{\theta}_{\text{true}}^\top \mathbf{x})) \right] = \mathbf{0},$$

then the local symmetry condition (8) holds, i.e., $\nabla \phi(\boldsymbol{\theta}^*) = \mathbf{0}$.

6 Practical Method: Validation-Tuned Synthetic Size (VTSS)

Our theory indicates that the common balancing rule $\tilde{n} = n_0 - n_1$ is not always optimal. In particular, Theorem 2 expresses the leading behavior of the excess risk as a function of the synthetic size \tilde{n} , implying that different choices of \tilde{n} (even when all are of the same order as $n_0 - n_1$) can yield materially different performance. While Theorem 2 also suggests an “optimal” \tilde{n} by minimizing the leading-term approximation, the resulting objective depends on population-level quantities, such as derivatives of the risk at $\boldsymbol{\theta}^*$, local symmetry $\nabla \phi(\boldsymbol{\theta}^*)$, and the generator-induced discrepancy $\nabla \psi(\boldsymbol{\theta}^*)$, that are not directly observable from finite samples. Hence, direct optimization is infeasible in practice.

Nevertheless, the theorem provides a clear operational message: *the choice of \tilde{n} is important*, and naive balancing may be suboptimal. Motivated by the fact that, in locally asymmetric regimes, consistency typically requires \tilde{n} to be close to $n_0 - n_1$ (equivalently, $\tilde{n}/(n_0 - n_1) \rightarrow 1$), we restrict attention to a neighborhood of the balancing choice. Specifically, we consider candidates

$$\tilde{n}(\gamma) = \text{round}(\gamma(n_0 - n_1)), \quad \gamma \in \Gamma,$$

where $\Gamma \subset \mathbb{R}_+$ is centered at 1. For each γ , we augment the training set to achieve a target minority count $n_1^{\text{tar}} = n_1 + \tilde{n}(\gamma)$, train the downstream classifier, and select the γ that minimizes the *balanced* validation loss. We refer to this procedure as *Validation-Tuned Synthetic Size (VTSS)* and summarize it in Algorithm 1.

Algorithm 1 Validation-Tuned Synthetic Size (VTSS)

Require: Imbalanced training set $\mathcal{D}_{\text{tr}} = \{(\mathbf{x}_i, y_i)\}_{i=1}^{n_0+n_1}$ with class counts (n_0, n_1) , validation set \mathcal{D}_{val} , candidate multipliers $\Gamma \subset \mathbb{R}_+$ (centered at 1), classifier training routine $\text{Fit}(\cdot)$, balanced log-loss $\widehat{L}_{\text{bal}}(\boldsymbol{\theta}; \mathcal{D}_{\text{val}}) = \frac{1}{2n_{0,\text{val}}} \sum_{i=1}^{n_{0,\text{val}}} \ell(\boldsymbol{\theta}; \mathbf{x}_i^{0,\text{val}}, 0) + \frac{1}{2n_{1,\text{val}}} \sum_{i=1}^{n_{1,\text{val}}} \ell(\boldsymbol{\theta}; \mathbf{x}_i^{1,\text{val}}, 1)$, synthetic generator $\text{Syn}(\cdot; n_1^{\text{tar}})$.

Ensure: Selected synthetic size \tilde{n}^{VTSS} (equivalently γ^{VTSS}) and $\hat{\boldsymbol{\theta}}^{\text{VTSS}}$.

- 1: Initialize best validation loss $L^{\text{VTSS}} \leftarrow +\infty$.
- 2: **for** each $\gamma \in \Gamma$ **do**
- 3: Compute candidate synthetic size $\tilde{n} \leftarrow \text{round}(\gamma(n_0 - n_1))$.
- 4: Set target minority count $n_1^{\text{tar}} \leftarrow n_1 + \tilde{n}$.
- 5: Augment training data: $\tilde{\mathcal{D}}_{\text{tr}}(\gamma) \leftarrow \text{Syn}(\mathcal{D}_{\text{tr}}; n_1^{\text{tar}})$.
- 6: Train classifier $\hat{\boldsymbol{\theta}}_\gamma \leftarrow \text{Fit}(\tilde{\mathcal{D}}_{\text{tr}}(\gamma))$.
- 7: Compute balanced validation log-loss $L_\gamma \leftarrow \widehat{L}_{\text{bal}}(\hat{\boldsymbol{\theta}}_\gamma; \mathcal{D}_{\text{val}})$.
- 8: **if** $L_\gamma < L^{\text{VTSS}}$ **then**
- 9: Update $L^{\text{VTSS}} \leftarrow L_\gamma$, $\gamma^{\text{VTSS}} \leftarrow \gamma$, $\hat{\boldsymbol{\theta}}^{\text{VTSS}} \leftarrow \hat{\boldsymbol{\theta}}_\gamma$.
- 10: **end if**
- 11: **end for**
- 12: Output $\tilde{n}^{\text{VTSS}} = \text{round}(\gamma^{\text{VTSS}}(n_0 - n_1))$ and $\hat{\boldsymbol{\theta}}^{\text{VTSS}}$.

7 Simulation Studies

In this section, we use controlled simulations to validate the theory developed above and to evaluate the practical benefits of Validation-Tuned Synthetic Size (VTSS) (Section 6). Our experiments are designed to demonstrate that the key qualitative predictions of our analysis hold in practice: synthetic augmentation helps under local asymmetry, but not under local symmetry. We also show that VTSS more reliably converts augmentation into improved downstream performance than the naive balancing rule $\tilde{n} = n_0 - n_1$.

7.1 Under Local Asymmetry

We first investigate simulations under local asymmetry, considering both cases with and without directional alignment. We further illustrate the theory under both realistic and inconsistent generators.

Classification Without Directional Alignment. We simulate an imbalanced binary classification problem in $d = 5$ where the majority class is i.i.d. $\mathbf{x} \mid y = 0 \sim \mathcal{N}(0, I_d)$ and the minority class is i.i.d. from a two-component Gaussian mixture: with probability 1/2, $\mathbf{x} \mid y = 1 \sim \mathcal{N}(\delta \mathbf{e}_1 + \frac{\xi}{2} \mathbf{e}_2, I_d)$ and with probability 1/2, $\mathbf{x} \mid y = 1 \sim \mathcal{N}(\delta \mathbf{e}_1 - \frac{\xi}{2} \mathbf{e}_2, I_d)$, with $\delta = 2.0$ and $\xi = 2.5$. Here \mathbf{e}_i denotes the d -dimensional standard basis vector. For each scale $m \in \{1, 2, 4, 8, 16\}$, we set $n_1 = 50m$ and $n_0 = 20n_1$, generate an imbalanced training set, and compare two SMOTE-based training strategies: (A) *naive balancing*, which oversamples the minority to exactly n_0 points via SMOTE (with $k = 5$ nearest neighbors),

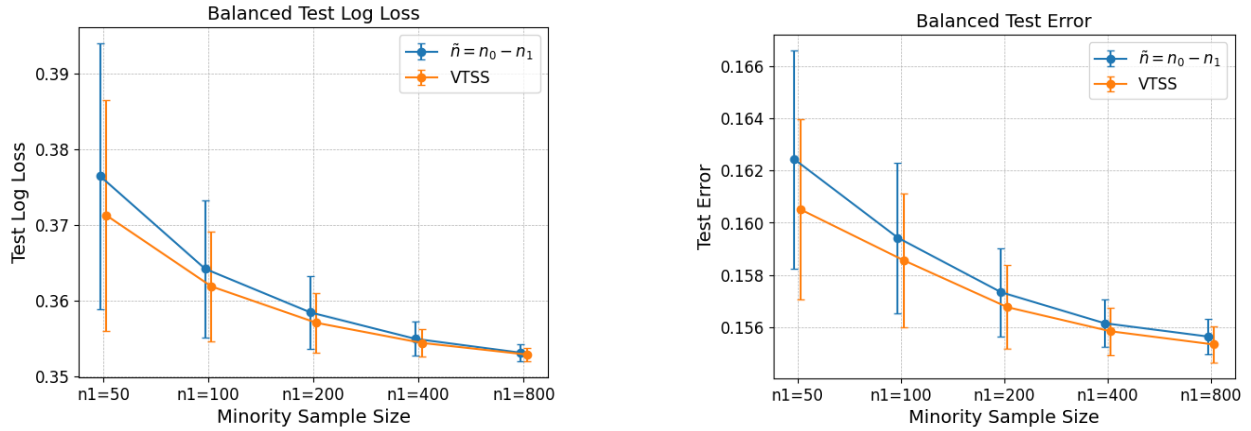


Figure 2: Balanced test performance under SMOTE with naive balancing versus VTSS.

and (B) *VTSS*, which selects \tilde{n} by minimizing balanced validation log-loss over a candidate grid (Section 6). In each case, we fit logistic regression on the SMOTE-augmented training data and evaluate performance on a large *balanced* test set generated from the true class-conditional distributions, with equal class sizes. Performance is reported using balanced log-loss and balanced test 0–1 error, averaged over 100 independent repetitions for each m .

As shown in Figure 2, both the balanced test log-loss and the balanced test error decrease as n_1 increases, reflecting the benefit of having more real minority observations. More importantly, VTSS consistently attains lower loss and error than the naive balancing rule and typically exhibits smaller variance, indicating that validation-based tuning yields a more stable procedure by avoiding over- or under-synthesis. The performance gap also narrows as n_1 grows: when the minority sample becomes sufficiently large, the tuned synthetic size tends to approach the naive target $n_0 - n_1$, so the incremental benefit diminishes. This setting does not exhibit strong directional alignment between the generator mismatch and the intrinsic imbalance effect, so our theory suggests limited gains from fine-tuning beyond near-balancing. In these simulations, VTSS does not underperform the naive choice $\tilde{n} = n_0 - n_1$. In practice, since one rarely knows a priori whether the minority sample size is already large enough for the gap to be negligible, VTSS provides a robust default.

Classification with Directional Alignment. To illustrate the directional-alignment phenomenon discussed in Section 4.3, we consider a 2D Gaussian setting as in Example 2, with imbalance ratio $n_0/n_1 = 20$. For n_1 varying from 6 to 3200, we set $n_0 = 20n_1$, draw majority samples $\mathbf{x} \mid y = 0 \sim \mathcal{N}(0, I_2)$ and minority samples $\mathbf{x} \mid y = 1 \sim \mathcal{N}(\boldsymbol{\mu}_1, I_2)$ with $\boldsymbol{\mu}_1 = (\mu, 0)$ and $\mu = 1$. We augment the training data with \tilde{n} synthetic points labeled as minority, generated from a biased but directionally aligned generator $\mathbf{x}_{\text{syn}} \sim \mathcal{N}(\boldsymbol{\mu}_s, I_2)$ with $\boldsymbol{\mu}_s = (a, 0)$ and $a = 0.5$. For each repetition (100 Monte Carlo runs per n_1), we also generate a fresh balanced test set of size 5000 per class from the true distributions. We compare two fixed synthetic-size rules: the naive balancing choice $\tilde{n} = n_0 - n_1$ and the bias-canceling choice $\tilde{n} = 4(n_0 - n_1)$ (from the analysis of Example 2). On each augmented training

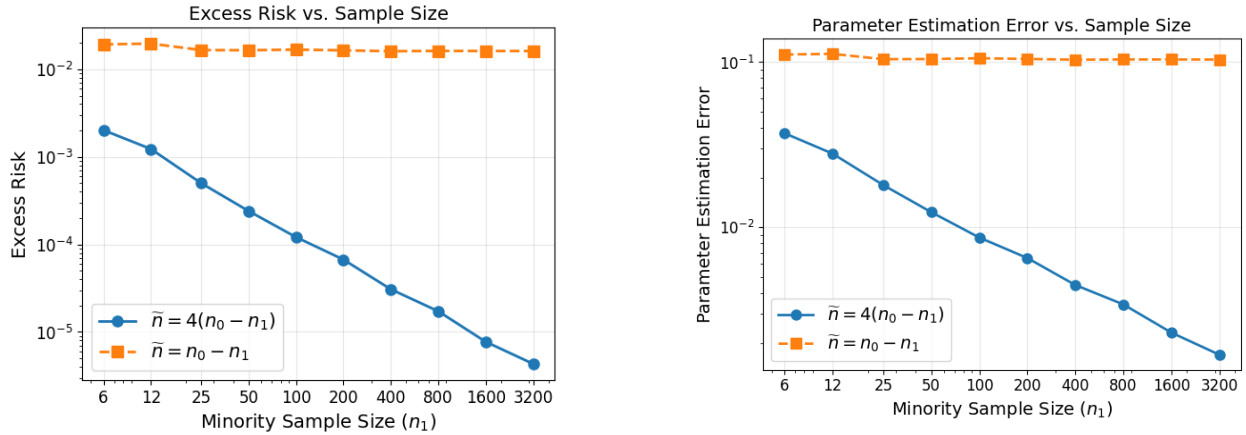


Figure 3: Balanced excess risk and parameter estimation error in a 2D Gaussian model with aligned synthetic bias.

set, we fit the linear predictor $\hat{\boldsymbol{\theta}} \in \mathbb{R}^2$ by least squares and evaluate (i) parameter error $\|\hat{\boldsymbol{\theta}} - \boldsymbol{\theta}^*\|_2$ and (ii) balanced excess risk $\mathcal{R}(\hat{\boldsymbol{\theta}}) - \mathcal{R}(\boldsymbol{\theta}^*)$, where $\mathcal{R}(\boldsymbol{\theta}) = \|\boldsymbol{\theta}\|_2^2 + \frac{1}{2}(\boldsymbol{\theta}^\top \boldsymbol{\mu}_1 - 1)^2$ and $\boldsymbol{\theta}^* = (\mu/(\mu^2 + 2), 0)$. Finally, we plot the mean and standard deviation of the excess risk and parameter error versus n_1 on log scales for the two choices of \tilde{n} .

The simulation in Figure 3 confirms the theoretical analysis in Example 2. When $\tilde{n} = 4(n_0 - n_1)$, both the balanced excess risk and the parameter error $\|\hat{\boldsymbol{\theta}} - \boldsymbol{\theta}^*\|_2$ decay to zero as the sample size grows, whereas under naive balancing they converge to a strictly positive level. This demonstrates that count balancing alone can be inconsistent in the presence of biased synthetic data.

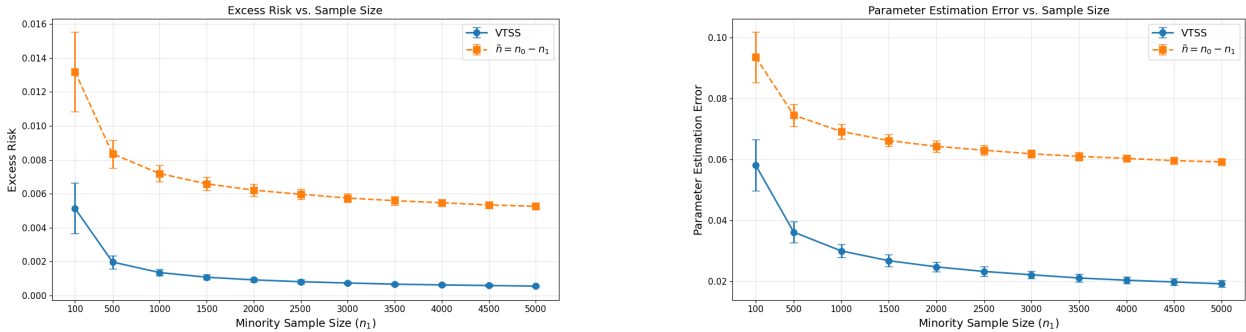


Figure 4: Excess risk and parameter error versus minority sample size under a 2D Gaussian mean-shift model (squared loss).

For directional alignment with a realistic and consistent synthetic generator (Section 4.2), we simulate the same 2D Gaussian setup as above under imbalance $n_0/n_1 = 20$ and squared loss. For $n_1 \in [100, 5000]$, we run 100 Monte Carlo repetitions, generating a fresh imbalanced training set and a balanced validation set of 1000 points per class. Synthetic minority samples are produced by a realistic, consistent, and directionally aligned generator:

for a requested synthetic size k , draw $\mathbf{x}_{\text{syn}} \sim \mathcal{N}(\boldsymbol{\mu}_{\text{syn}}, I_2)$ with

$$\boldsymbol{\mu}_{\text{syn}} = (1 - (\log n_1)^{-1/2}) \boldsymbol{\mu}_1,$$

so that the synthetic mean approaches $\boldsymbol{\mu}_1$ as n_1 increases while remaining aligned with $\boldsymbol{\mu}_1$. We compare VTSS with the naive balancing rule $\tilde{n} = n_0 - n_1$, fit a least-squares predictor on the augmented training data, and evaluate both methods using population excess risk $\mathcal{R}(\hat{\boldsymbol{\theta}}) - \mathcal{R}(\boldsymbol{\theta}^*)$ and parameter error $\|\hat{\boldsymbol{\theta}} - \boldsymbol{\theta}^*\|_2$, reporting mean \pm standard deviation over repetitions as functions of n_1 .

The results are shown in Figure 4. Across all values of n_1 , VTSS achieves substantially smaller errors and a faster decay rate, supporting our theory that, under a realistic but consistent generator, directional information can be exploited to select \tilde{n} that outperforms naive balancing. In contrast to Figure 2, where the gap between the two methods diminishes as n_1 grows, here the gap remains substantial, highlighting the effect of directional alignment.

7.2 Under Local Symmetry

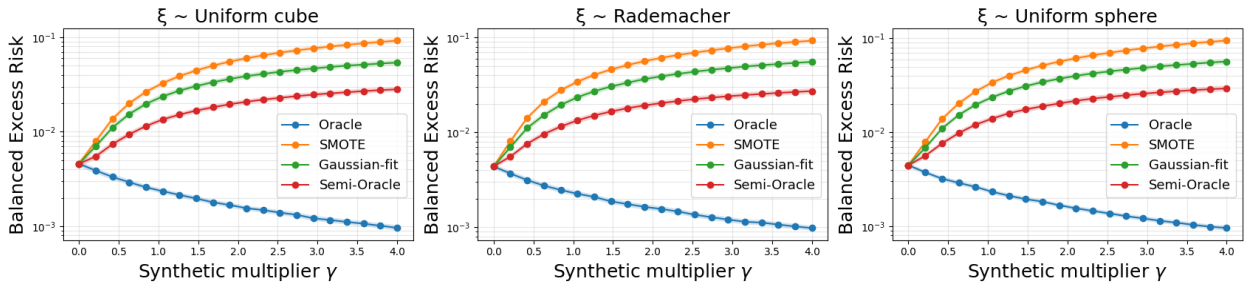


Figure 5: Balanced excess risk $\mathcal{R}(\hat{\boldsymbol{\theta}}) - \mathcal{R}(\boldsymbol{\theta}^*)$ (log scale) versus the synthetic-size multiplier γ .

To further illustrate local symmetry (Section 5), we conduct a simulation study based on the mean-shift model in Example 3. We generate imbalanced binary data in dimension $d = 20$ from

$$\mathbf{x} \mid y = 1 \sim \boldsymbol{\mu} + \boldsymbol{\xi}, \quad \mathbf{x} \mid y = 0 \sim -\boldsymbol{\mu} + \boldsymbol{\xi},$$

where $\boldsymbol{\mu} = \delta \mathbf{e}_1$ with $\delta = 1$ and $\mathbf{e}_1 = (1, 0, \dots, 0)^\top$. Here $\boldsymbol{\xi}$ has mean zero and identity covariance. We consider three choices of $\boldsymbol{\xi}$: (i) Uniform cube with independent coordinates $\xi_j \sim \text{Unif}[-\sqrt{3}, \sqrt{3}]$, (ii) Rademacher with $\xi_j \in \{-1, +1\}$ equally likely, and (iii) Uniform-on-sphere obtained by sampling $\mathbf{g} \sim \mathcal{N}(0, I_d)$ and setting $\boldsymbol{\xi} = \sqrt{d} \mathbf{g} / \|\mathbf{g}\|$. We start from an imbalanced training sample with $n_1 = 100$ and $n_0 = 2000$, and augment the minority class with $\tilde{n} = \text{round}(\gamma(n_0 - n_1))$ synthetic samples, where γ ranges over 20 values in $[0, 4]$. We fit a linear predictor under squared loss on the augmented sample and report the balanced excess risk $\mathcal{R}(\hat{\boldsymbol{\theta}}) - \mathcal{R}(\boldsymbol{\theta}^*)$, where $\boldsymbol{\theta}^* = \boldsymbol{\mu} / (1 + \|\boldsymbol{\mu}\|_2^2)$ and $\mathcal{R}(\boldsymbol{\theta})$ is evaluated in closed form under the population model. We compare four synthetic generators: (i) **Oracle**, which draws synthetic points from the true minority distribution $\boldsymbol{\mu} + \boldsymbol{\xi}$; (ii) **SMOTE**, which interpolates

between minority neighbors (with $k = 5$); (iii) **Gaussian-fit**, which samples from $\mathcal{N}(\hat{\mu}_1, \hat{\Sigma})$ using the empirical minority mean and covariance estimate; and (iv) **Semi-Oracle**, which samples ξ from the true noise distribution but centers at the empirical minority mean $\hat{\mu}_1$ (i.e., $\hat{\mu}_1 + \xi$). Results are averaged over 100 Monte Carlo repetitions, and we plot the mean balanced excess risk across repetitions as a function of γ on a log scale.

The results in Figure 5 align with the theoretical analysis. In the mean-shift setting, the majority–minority difference cancels at the balanced optimum ($\nabla\phi(\boldsymbol{\theta}^*) = 0$), so adding synthetic data from a realistic generator cannot reduce this part of the error. Instead, any mismatch between the synthetic and true minority distributions introduces bias and can only worsen balanced excess risk. Empirically, realistic generators, including the Semi-Oracle generator that is already close to the truth, fail to improve performance and typically degrade it as more synthetic samples are added. In contrast, only the Oracle generator improves monotonically with increasing γ , reflecting that it avoids generator-induced mismatch and helps by adding correctly distributed minority samples.

We also examine the VTSS-selected multiplier γ^* in the same mean-shift setup. Rather than sweeping γ to plot excess-risk curves, we focus on the empirical distribution of the minimizer γ^* . For each noise distribution ξ (Uniform cube, Rademacher, Uniform sphere), we run 500 repetitions. In each repetition, we generate a fresh balanced validation set with 2000 samples per class and tune over a grid of 200 equally spaced candidates $\gamma \in [0, 2]$ (including $\gamma = 0$). For each candidate γ and each generator, we fit the least-squares predictor on the augmented training set and set γ^* to the minimizer of the validation loss. Figure 6 reports the empirical distribution of γ^* . VTSS selects a very small γ^* in the vast majority of runs and frequently chooses $\gamma^* = 0$ exactly. The intuition is that when synthetic augmentation provides no genuine benefit and can introduce mismatch-induced bias, the balanced validation objective typically does not decrease as γ increases. Hence, the minimizer is attained at (or near) the boundary $\gamma = 0$, allowing the procedure to automatically opt out of synthetic data in this regime.

To further demonstrate a regime where class imbalance is not the bottleneck, we consider the sigmoid Bernoulli logistic model in Example 4 with dimension $d = 20$. We let $\mathbf{v} = \mathbf{e}_1$ and $\boldsymbol{\theta}_{\text{true}} = c\mathbf{v}$ with $c = 1$, and generate covariates as $\mathbf{x} = T\mathbf{v} + W$, where $T \in \{-a, b\}$ with $a = 5$, $b = 1$, and $\Pr(T = -a) = \alpha$ chosen to ensure bias cancellation. The noise W is orthogonal to \mathbf{v} (its first coordinate is identically zero) and has a symmetric, non-Gaussian mixture distribution in the remaining coordinates: $W_{2:d} = \mathbf{z} + s\boldsymbol{\mu}$ with $\mathbf{z} \sim \mathcal{N}(0, I)$, $s \in \{\pm 1\}$ equally likely, and $\boldsymbol{\mu}$ having its first three entries equal to 2.5 (others zero), making Gaussian-fit imperfect. Labels are drawn as $y \in \{0, 1\}$ with $\Pr(y = 1 \mid \mathbf{x}) = \sigma(\boldsymbol{\theta}_{\text{true}}^\top \mathbf{x})$. For each of 100 repetitions, we sample $n_{\text{train}} = 5000$ i.i.d. training pairs (\mathbf{x}, y) (with random realized class counts), define the minority class as the label with fewer observations, and augment only that minority class to size $n_1 + \tilde{n}$, where $\tilde{n} = \text{round}(\gamma(n_0 - n_1))$ and γ ranges over $[0, 2]$. We compare three generators for minority augmentation: SMOTE (nearest-neighbor interpolation with $k = 5$), Gaussian-fit (sampling from a fitted Gaussian using the minority empirical mean and covariance with a small ridge), and an Oracle generator that draws fresh (\mathbf{x}, y) from the true model and keeps only minority-labeled points. For each augmented dataset, we fit logistic regression and report (i) balanced excess logistic risk relative to $\boldsymbol{\theta}^*$

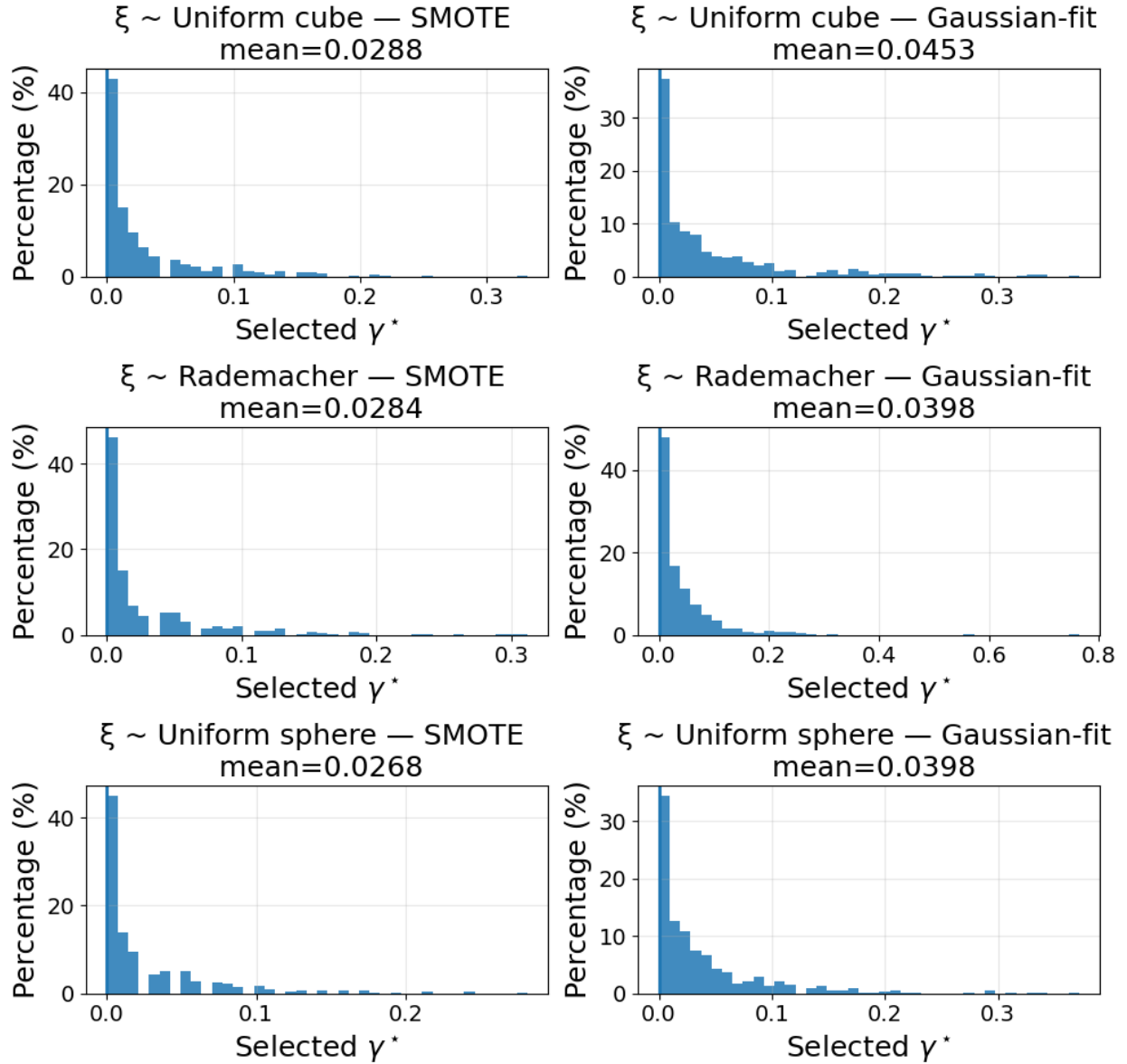


Figure 6: Histograms of the selected synthetic multiplier γ^* chosen by VTSS.

and (ii) parameter error $\|\hat{\boldsymbol{\theta}} - \boldsymbol{\theta}^*\|_2$, where $\boldsymbol{\theta}^*$ is obtained by fitting the same model on a large balanced sample of 20,000 per class.

Figure 7 shows that, for realistic generators such as SMOTE and Gaussian-fit, increasing γ does not reduce balanced excess risk or parameter error; in fact, performance typically worsens. In contrast, the Oracle generator improves monotonically, as expected.

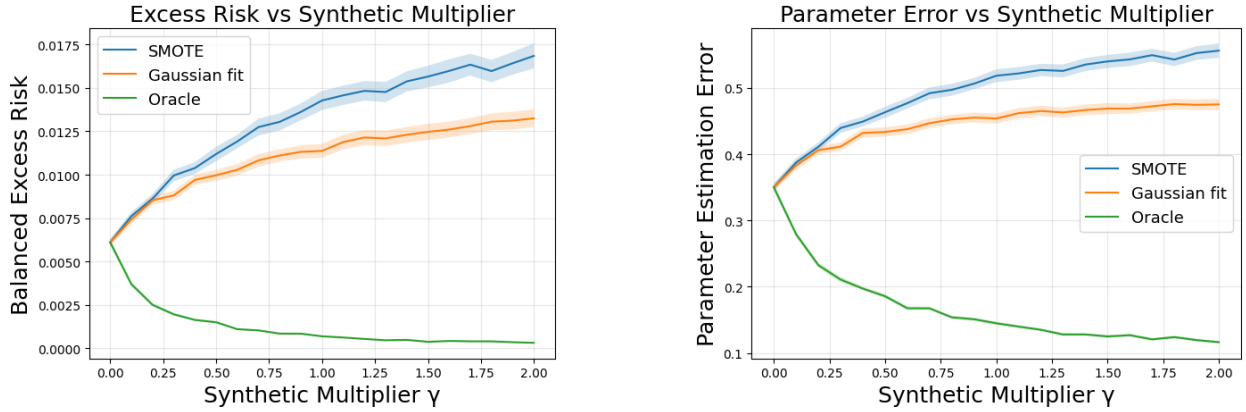


Figure 7: Synthetic augmentation does not help under a bias-cancellation sigmoid Bernoulli model.

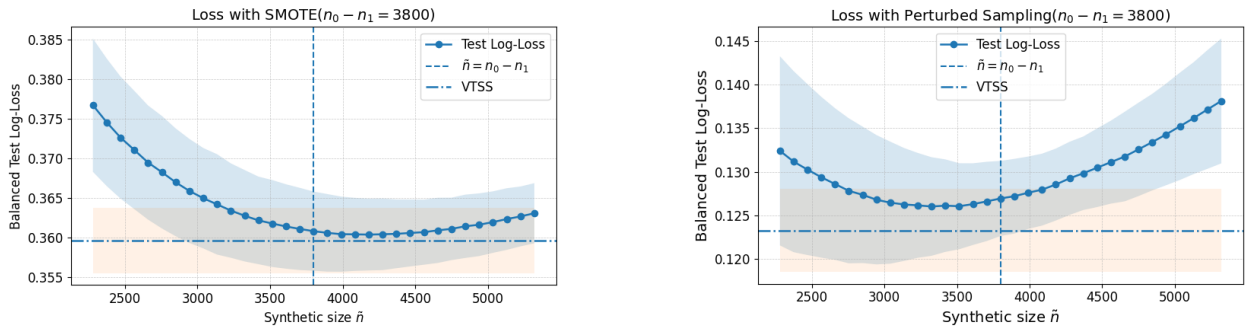


Figure 8: Balanced test log-loss as a function of the synthetic size \tilde{n} . **Left:** logistic regression with SMOTE as the synthetic generator. **Right:** kernel logistic regression with perturbed sampling as the synthetic generator.

7.3 Further Evaluation of VTSS

In this subsection, we further illustrate the advantage of VTSS by plotting the test loss as a function of the synthetic size \tilde{n} and comparing it with the loss achieved by VTSS. We consider two configurations.

Linear classification (SMOTE + logistic regression). We generate imbalanced training data in $d = 5$ with ratio $r = n_0/n_1 = 20$ (in the plotted curve, $n_1 = 200$, $n_0 = 4000$, and $n_0 - n_1 = 3800$). The majority class is $\mathcal{N}(0, I)$, while the minority class is a balanced two-component Gaussian mixture, with each component having covariance I and means $\mu_{\pm} = \delta e_1 \pm \frac{\xi}{2} e_2$. For each of 100 repetitions, we sweep \tilde{n} over a grid induced by $\gamma \in [0.6, 1.4]$ via $\tilde{n} = \text{round}(\gamma(n_0 - n_1))$, apply SMOTE to reach minority size $n_1 + \tilde{n}$, fit logistic regression, and evaluate balanced test log-loss on a fixed balanced test set (10,000 per class). VTSS chooses \tilde{n} in each repetition by minimizing the same balanced log-loss on a validation set, and we plot its average test loss as a horizontal reference line.

Nonlinear classification (perturbed sampling + kernel logistic). We use a non-Gaussian data-generating process in $d = 5$. For the majority class $y = 0$, we first draw a mixture indicator $z \sim \text{Bernoulli}(0.30)$, then sample the first two coordinates from a correlated Gaussian $(x_1, x_2) \sim \mathcal{N}\left((1.5 \cdot z, 0), \begin{pmatrix} 1 & 0.5 \\ 0.5 & 1 \end{pmatrix}\right)$, and sample the remaining coordinates i.i.d. as $x_{3:5} \sim \mathcal{N}(0, I_3)$. For the minority class $y = 1$, we generate a noisy ring in the (x_1, x_2) -plane by drawing an angle $\omega \sim \text{Unif}[0, 2\pi]$ and radius $r = 2.2 + \varepsilon_r$ with $\varepsilon_r \sim \mathcal{N}(0, 0.12^2)$, then setting

$$x_1 = \delta + r \cos \omega + \varepsilon_1, \quad x_2 = r \sin \omega + \varepsilon_2,$$

with $\varepsilon_1, \varepsilon_2 \sim \mathcal{N}(0, 0.08^2)$ and $\delta = 4.8$. The remaining coordinates are small Gaussian noise $x_{3:5} \sim \mathcal{N}(0, 0.08^2 I_3)$. This simulation is a controlled nonlinear-boundary benchmark, designed to test whether VTSS can tune synthetic size when the generator introduces distributional blur. We embed the 2D structure in $d = 5$ by adding nuisance coordinates, reflecting the common setting where only a subset of features drives class separation.

Synthetic data are generated by perturbed resampling: bootstrap minority points and add Gaussian jitter $\mathcal{N}(0, I)$. We train an RBF-kernel probabilistic classifier, sweep $\tilde{n} = \text{round}(\gamma(n_0 - n_1))$ over $\gamma \in [0.6, 1.4]$, and let VTSS pick \tilde{n} via validation minimization in each repetition.

In both configurations of Figure 8, the empirical curves confirm the theoretical insight that, although the naive balancing choice $\tilde{n} = n_0 - n_1$ often lies near the optimum, it is generally not the loss-minimizing synthetic size. Moreover, VTSS, which selects \tilde{n} by minimizing balanced validation loss on each dataset, achieves substantially lower average loss than any single fixed choice of \tilde{n} over 100 repetitions. This highlights the benefit of data-dependent tuning around a theory-guided target.

8 Discussion

This paper develops a unified risk-based theory for synthetic minority augmentation in imbalanced classification under a balanced evaluation objective. We derive an excess-risk decomposition that separates imbalance-induced objective distortion from generator-induced mismatch, and show how the synthetic size \tilde{n} governs the resulting bias-variance trade-off. The theory identifies two regimes: under local asymmetry, augmentation can help, but the optimal \tilde{n} depends on generator quality and may deviate from naive full balancing (especially under directional alignment); under local symmetry, imbalance is not the first-order bottleneck, so realistic augmentation typically cannot help and may hurt by amplifying mismatch. These insights motivate Validation-Tuned Synthetic Size (VTSS), which selects \tilde{n} using balanced validation loss to capture gains when tuning matters while avoiding oversynthesis when augmentation is unhelpful.

Our analysis focuses on a classical low-dimensional asymptotic regime with fixed covariate dimension d . Extending the framework to high-dimensional settings, where both downstream learning and generator mismatch can change qualitatively, and where mismatch may worsen due to curse-of-dimensionality effects, is an important direction. In such regimes,

understanding how mismatch scales with d , how the bias–variance trade-off shifts, and how to adapt VTSS when validation is noisy or limited remain open problems.

Our results also clarify settings where oversampling is less likely to help even in low dimensions. For likelihood-based generative discriminant models such as LDA, class imbalance primarily enters through an explicit prior term, so balanced or cost-sensitive operating points can often be achieved by adjusting priors at prediction time rather than altering the training sample composition. Moreover, because these methods are sensitive to moment misspecification, synthetic samples can be counterproductive if they introduce even mild mean or covariance distortions.

A key message is that the direction of generator mismatch matters. This connects naturally to guided generative modeling (e.g., guided diffusion or instruction-tuned LLMs): if guidance can steer the dominant mismatch component toward the imbalance-relevant direction, augmentation becomes more effective and modest deviations from naive balancing can yield measurable gains. This suggests future work on augmentation-aware generator training that optimizes not only sample realism but also mismatch in the directions most relevant to the downstream balanced risk.

References

T. Ahmad, M. M. Kalan, F. Portier, and G. Stupler. Concentration and excess risk bounds for imbalanced classification with synthetic oversampling. *arXiv preprint arXiv:2510.20472*, 2025.

A. Bougaham, M. El Adoui, I. Linden, and B. Frénay. Composite score for anomaly detection in imbalanced real-world industrial dataset. *Machine Learning*, 113(7):4381–4406, 2024.

C. Bunkhumpornpat, K. Sinapiromsaran, and C. Lursinsap. Safe-level-SMOTE: Safe-level-synthetic minority over-sampling technique for handling the class imbalanced problem. In *Pacific-Asia Conference on Knowledge Discovery and Data Mining*, pages 475–482. Springer, 2009.

C. Bunkhumpornpat, K. Sinapiromsaran, and C. Lursinsap. Dbsmote: density-based synthetic minority over-sampling technique. *Applied Intelligence*, 36(3):664–684, 2012.

N. V. Chawla, K. W. Bowyer, L. O. Hall, and W. P. Kegelmeyer. SMOTE: Synthetic minority over-sampling technique. *Journal of Artificial Intelligence Research*, 16:321–357, 2002.

W. Chen, K. Yang, Z. Yu, Y. Shi, and C. P. Chen. A survey on imbalanced learning: latest research, applications and future directions. *Artificial Intelligence Review*, 57(6):137, 2024a.

Y. Chen, R. Calabrese, and B. Martin-Barragan. Interpretable machine learning for imbalanced credit scoring datasets. *European Journal of Operational Research*, 312(1):357–372, 2024b.

B. Efron and R. J. Tibshirani. *An introduction to the bootstrap*. Chapman and Hall/CRC, 1994.

P. Eigenschink, T. Reutterer, S. Vamosi, R. Vamosi, C. Sun, and K. Kalcher. Deep generative models for synthetic data: A survey. *IEEE Access*, 11:47304–47320, 2023.

C. Faviez, X. Chen, N. Garcelon, A. Neuraz, B. Knebelmann, R. Salomon, S. Lyonnet, S. Saunier, and A. Burgun. Diagnosis support systems for rare diseases: a scoping review. *Orphanet Journal of Rare Diseases*, 15(1):94, 2020.

I. J. Goodfellow, J. Pouget-Abadie, M. Mirza, B. Xu, D. Warde-Farley, S. Ozair, A. Courville, and Y. Bengio. Generative adversarial nets. *Advances in neural information processing systems*, 27, 2014.

H. Han, W. Y. Wang, and B. H. Mao. Borderline-SMOTE: A new over-sampling method in imbalanced data sets learning. In *International Conference on Intelligent Computing*, pages 878–887. Springer, 2005.

H. He, Y. Bai, E. A. Garcia, and S. Li. ADASYN: Adaptive synthetic sampling approach for imbalanced learning. In *2008 IEEE International Joint Conference on Neural Networks (IEEE World Congress on Computational Intelligence)*, pages 1322–1328. IEEE, 2008.

J. Ho, A. Jain, and P. Abbeel. Denoising diffusion probabilistic models. *Advances in neural information processing systems*, 33:6840–6851, 2020.

L.-C. Hung, Y.-H. Hu, C.-F. Tsai, and M.-W. Huang. A dynamic time warping approach for handling class imbalanced medical datasets with missing values: A case study of protein localization site prediction. *Expert systems with applications*, 192:116437, 2022.

N. Keret and A. Shojaie. Glm inference with ai-generated synthetic data using misspecified linear regression. *arXiv preprint arXiv:2503.21968*, 2025.

D. P. Kingma and M. Welling. Auto-encoding variational Bayes. *arXiv preprint arXiv:1312.6114*, 2013.

I. Ktena, O. Wiles, I. Albuquerque, S.-A. Rebuffi, R. Tanno, A. G. Roy, S. Azizi, D. Belgrave, P. Kohli, T. Cemgil, et al. Generative models improve fairness of medical classifiers under distribution shifts. *Nature Medicine*, 30(4):1166–1173, 2024.

P. Lyu, Z. Ma, L. Zhang, and A. R. Zhang. Bias-corrected data synthesis for imbalanced learning. *arXiv preprint arXiv:2510.26046*, 2025.

R. Nakada, Y. Xu, L. Li, and L. Zhang. Synthetic oversampling: Theory and a practical approach using llms to address data imbalance. *arXiv preprint arXiv:2406.03628*, 2024.

G. Papamakarios, E. Nalisnick, D. J. Rezende, S. Mohamed, and B. Lakshminarayanan. Normalizing flows for probabilistic modeling and inference. *Journal of Machine Learning Research*, 22(57):1–64, 2021.

C. Piciarelli, P. Mishra, and G. L. Foresti. Supervised anomaly detection with highly imbalanced datasets using capsule networks. *International Journal of Pattern Recognition and Artificial Intelligence*, 35(08):2152010, 2021.

O. Räisä, J. Jälkö, and A. Honkela. On consistent bayesian inference from synthetic data. *Journal of Machine Learning Research*, 26(74):1–65, 2025.

A. J. Rodriguez-Almeida, H. Fabelo, S. Ortega, A. Deniz, F. J. Balea-Fernandez, E. Quevedo, C. Soguero-Ruiz, A. M. Wägner, and G. M. Callico. Synthetic patient data generation and evaluation in disease prediction using small and imbalanced datasets. *IEEE journal of biomedical and health informatics*, 27(6):2670–2680, 2022.

R. Roy, D. Tiwari, and A. Pandey. Frauddiffuse: Diffusion-aided synthetic fraud augmentation for improved fraud detection. In *Proceedings of the 5th ACM International Conference on AI in Finance*, pages 90–98, 2024.

M. Salmi, D. Atif, D. Oliva, A. Abraham, and S. Ventura. Handling imbalanced medical datasets: review of a decade of research. *Artificial intelligence review*, 57(10):273, 2024.

Y. Song, J. Sohl-Dickstein, D. P. Kingma, A. Kumar, S. Ermon, and B. Poole. Score-based generative modeling through stochastic differential equations. *arXiv preprint arXiv:2011.13456*, 2020.

I. Stanton, K. Munir, A. Ikram, and M. El-Bakry. Data augmentation for predictive maintenance: Synthesising aircraft landing gear datasets. *Engineering Reports*, 6(12):e12946, 2024.

S. Subudhi and S. Panigrahi. Effect of class imbalancedness in detecting automobile insurance fraud. In *2018 2nd International Conference on Data Science and Business Analytics (ICDSBA)*, pages 528–531. IEEE, 2018.

X. Tian and X. Shen. Conditional data synthesis augmentation. *arXiv preprint arXiv:2504.07426*, 2025.

G. Tong and J. Shen. Financial transaction fraud detector based on imbalance learning and graph neural network. *Applied Soft Computing*, 149:110984, 2023.

J. Wang, K. Wang, Y. Yu, Y. Lu, W. Xiao, Z. Sun, F. Liu, Z. Zou, Y. Gao, L. Yang, et al. Self-improving generative foundation model for synthetic medical image generation and clinical applications. *Nature Medicine*, 31(2):609–617, 2025.

E. Xia and J. M. Klusowski. Classification imbalance as transfer learning. *arXiv preprint arXiv:2601.10630*, 2026.

H. Zhang, M. Cisse, Y. N. Dauphin, and D. Lopez-Paz. Mixup: Beyond empirical risk minimization. *arXiv preprint arXiv:1710.09412*, 2017.